

# Two-Stroke Optimization Scheme for Mesoscopic Refrigerators

Paul Menczel, Tuomas Pyhäranta, Christian Flindt, and Kay Brandner  
*Department of Applied Physics, Aalto University, 00076 Aalto, Finland*

Refrigerators use a thermodynamic cycle to move thermal energy from a cold reservoir to a hot one. Implementing this operation principle with mesoscopic components has recently emerged as a promising strategy to control heat currents in micro and nano systems for quantum technological applications. Here, we combine concepts from stochastic and quantum thermodynamics with advanced methods of optimal control theory to develop a universal optimization scheme for such small-scale refrigerators. Covering both the classical and the quantum regime, our theoretical framework provides a rigorous procedure to determine the periodic driving protocols that maximize either cooling power or efficiency. As a main technical tool, we decompose the cooling cycle into two strokes, which can be optimized one by one. In the regimes of slow or fast driving, we show how this procedure can be simplified significantly by invoking suitable approximations. To demonstrate the practical viability of our scheme, we determine the exact optimal driving protocols for a quantum microcooler, which can be realized experimentally with current technology. Our work provides a powerful tool to develop optimal design strategies for engineered cooling devices and it creates a versatile framework for theoretical investigations exploring the fundamental performance limits of mesoscopic thermal machines.

## I. INTRODUCTION

With the rapid advance of quantum technologies during the last decade, the search for new strategies to overcome the challenges of thermal management at low temperatures and small length scales has become a subject of intense research [1–5]. Solid-state quantum devices based on, for example, superconducting circuits require operation temperatures in the range of millikelvins, which must currently be upheld with massive and costly cryogenic equipment. These systems are among the most promising candidates to realize a large-scale quantum computer [6–8]; they also provide a versatile platform for the design of accurately tunable thermal instruments that can be implemented on chip and thus make it possible to control the heat flow between individual components of complex quantum circuits [9–15]. This technology could significantly simplify the operation of quantum devices by enabling the selective cooling of their functional degrees of freedom.

Mesoscopic refrigerators play a promising role in the development of integrated quantum cooling solutions. Mimicking the cyclic operation principle of their macroscopic counterparts, which are used in everyday appliances such as freezers and air conditioners, these devices use periodic driving fields to transfer heat from a cold object to a hot one [16–27]. Their basic working mechanism can be understood as a two-stroke process. In the first stroke, a certain amount of heat is absorbed from the cold body into a working system, which acts as a container for thermal energy. The second stroke uses the power input from the external driving field to inject the acquired heat into a hot reservoir and restore the initial state of the working system as illustrated in Fig. 1.

The thermodynamic performance of this cycle is crucially determined by the driving protocol that is applied to the working system. Finding its optimal shape is vital for practical applications and, at the same time, consti-

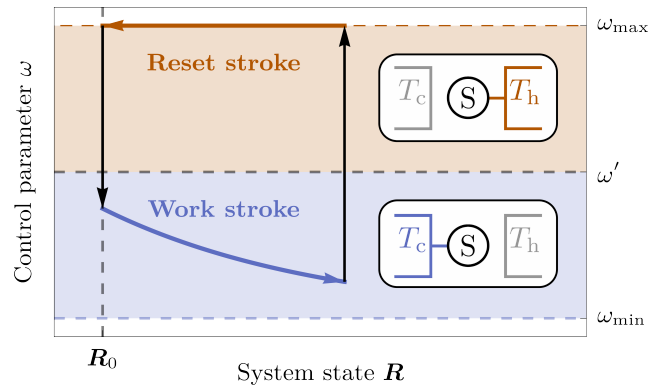


Figure 1. Thermodynamic operation cycle of a two-stroke refrigerator. Depending on whether the value of the control parameter  $\omega$  is smaller or larger than a given threshold  $\omega'$ , the working system  $S$  couples to a reservoir with temperature  $T_c$  or to a hotter one with temperature  $T_h > T_c$ . The possible values of the control parameter are delimited by  $\omega_{\min}$  and  $\omega_{\max}$ . In the work stroke, heat is transferred from the cold reservoir to the working system (blue arrow). The reset stroke restores the initial state  $R_0$ , while  $S$  is in contact with the hot reservoir (red arrow). The two strokes are connected by instantaneous jumps of the control parameter (black arrows).

tutes a formidable theoretical task. In fact, finding optimal strategies to control periodic thermodynamic processes in small-scale systems is a longstanding problem in both stochastic [28–35] and quantum thermodynamics [36–41], which involves three major challenges. First, the intricate interdependence between state and control variables that governs the dynamics of mesoscopic devices leads to constraints that can usually not be solved explicitly. Second, thermodynamic figures of merit such as cooling power are typically unbounded functions of external control parameters. The optimal protocol is then determined by the boundaries of the admissible parameter space and cannot be found from Euler-Lagrange equa-

tions, a situation known as a bang-bang scenario [42–44]. Third, a periodic mode of operation requires that the initial configuration of the device is restored after a given cycle time [40, 45]. This constraint effectively renders the optimization problem non-local in time, since any change of the driving protocol during the cycle affects the final state of the working system.

In this article, we show how these problems can be handled in three successive steps forming a universal scheme that makes it possible to maximize both the cooling power and the efficiency of mesoscopic refrigerators. The key idea of our method is to divide the refrigeration cycle into two strokes, which can be optimized one by one after fixing suitable boundary conditions, see Fig. 1. Dynamical constraints are thereby included through time-dependent Lagrange multipliers and bang-bang type protocols are taken into account systematically by applying Pontryagin’s minimum principle [42, 46] as we explain in the following. This two-step procedure effectively fixes the shape of the optimal driving protocol. The extracted heat, which initially depends on the entire control protocol, is thus reduced to an ordinary function of time-independent variational parameters, which can be optimized with standard techniques.

To illustrate our general formalism, we analyze a semiclassical model of a realistic quantum microcooler based on superconducting circuits, which can be implemented with current experimental technology [15, 38]. This application demonstrates the practical viability of our new scheme. Moreover, since the optimization of our model can be performed essentially through analytical calculations, it also provides valuable insights into characteristic features of optimal cooling cycles in mesoscopic systems.

The scope of our two-stroke framework is not limited to elementary models that can be treated exactly. By contrast, owing to its general structure, our scheme can be combined with a variety of established dynamical approximation methods to become an even more powerful theoretical tool. In this way, a physically transparent picture can also be obtained of complicated optimization problems, for which even numerically exact solutions would be practically out of reach. In the second part of our paper, we show how such a perturbative approach can be implemented for the limiting regimes of slow and fast driving. We round off our work by applying these techniques to determine the optimal working conditions of a superconducting microcooler in the full quantum regime.

Our manuscript is organized as follows. In Sec. II, we establish our two-stroke optimization scheme, which provides the general basis for this paper. In Sec. III, we use this framework to optimize the performance of a realistic model for a quantum microcooler in the semiclassical regime. We further develop our general theory in Sec. IV by incorporating two key dynamical approximation methods. In Sec. V, we apply these techniques to extend the semiclassical case study of Sec. III to the coherent regime. Finally, we conclude and discuss the new perspectives opened by our work in Sec. VI. Appen-

dices A and B contain further technical details of our calculations.

## II. GENERAL SCHEME

### A. Setup

A two-stroke refrigerator consists of three basic components: two reservoirs at different temperatures  $T_c$  and  $T_h > T_c$  and a controlled working system [47, 48]. We start by developing our general scheme before moving on to specific applications in Secs. III and V. The internal state of the working system is described by a vector of  $N$  independent variables  $\mathbf{R}_t$ , which follows the time evolution equation

$$\dot{\mathbf{R}}_t = \mathbf{F}[\mathbf{R}_t, \omega_t] \quad (1)$$

with dots indicating time-derivatives throughout. The generator  $\mathbf{F}$  thereby depends on the specific architecture of the device and it is assumed to be local in time, i.e., it only depends on the state vector  $\mathbf{R}_t$  and the driving protocol  $\omega_t$  at time  $t$ . It may, however, be a non-linear function of these variables. The external parameter  $\omega_t$  plays a three-fold role; it controls the dynamics of the state vector, modulates the internal energy landscape of the working system, and it regulates the coupling to the reservoirs [49].

The key idea of our two-stroke scheme is to disentangle these effects. To this end, we assume that the working system is connected either to the cold or the hot reservoir depending on whether  $\omega_t$  is smaller or larger than a given threshold value  $\omega'$ . A thermodynamic cooling cycle can then be realized as illustrated in Fig. 1. In the work stroke, the control parameter  $\omega_t$  changes continuously and does not exceed the threshold  $\omega'$ . Thus, the working system is constantly coupled to the cold reservoir, from which it has picked up the heat

$$\mathcal{Q}_c[\omega_t] \equiv \int_0^{\tau'} Q[\mathbf{R}_t, \omega_t] dt \quad (2)$$

by the end of the stroke. Here,  $Q[\mathbf{R}_t, \omega_t]$  is the instantaneous heat flux flowing into the system. Throughout this paper, we use calligraphic letters to denote functionals, which depend on the complete driving protocol  $\omega_t$ , for example the left hand side of (2). At the switching time  $\tau'$ ,  $\omega_t$  is abruptly raised above the threshold  $\omega'$ . This operation initializes the reset stroke, during which the control parameter follows a continuous trajectory without falling below  $\omega'$ . Hence, the system is coupled to the hot reservoir throughout this stroke, which restores the initial state of the system and releases the heat

$$\mathcal{Q}_h[\omega_t] \equiv - \int_{\tau'}^{\tau} Q[\mathbf{R}_t, \omega_t] dt. \quad (3)$$

The cycle is completed at the time  $\tau$  by instantaneously resetting the control parameter to its initial value.

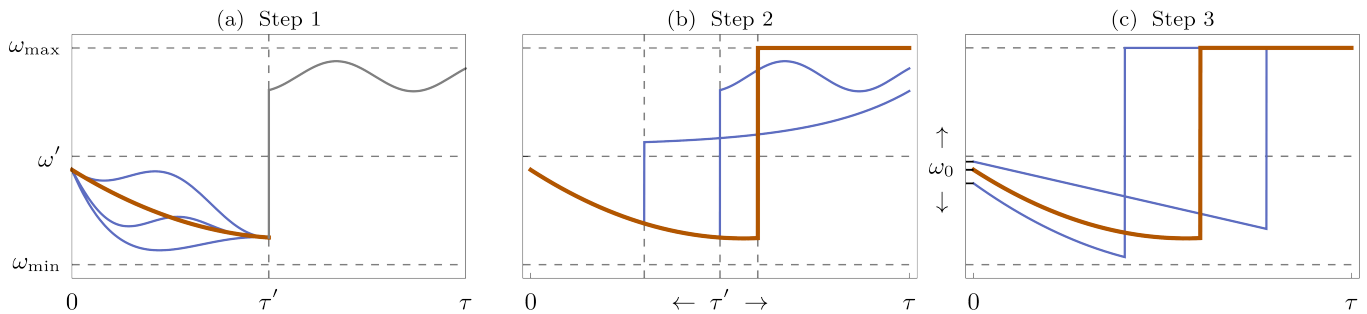


Figure 2. Maximizing the cooling power of a two-stroke refrigerator in three steps. (a) In step 1, the optimal work protocol (red line) is determined by variation of the functional (5) for a fixed switching time  $\tau'$ . Adding small displacements (blue lines) to the optimal protocol can only reduce the extracted heat. The reset stroke protocol (gray line) does not play a role here. (b) Step 2 optimizes the reset protocol such that the initial state of the system is restored, while keeping the optimal work stroke with given initial conditions fixed. The optimal reset stroke (in red) is thereby distinguished by having the latest possible switching time  $\tau'$ . The blue lines are examples of non-optimal reset stroke protocols with earlier switching times. (c) The initial values are determined in step 3, which completes the optimal protocol (in red). It is here compared to the protocols in blue, which are obtained by following steps 1 and 2 for different initial conditions and yield a lower heat extraction.

The specific form of the function  $Q[\mathbf{R}_t, \omega_t]$  is determined by the architecture of the refrigerator. For example, if the working system can be described as an open quantum system in the weak coupling regime, this quantity can universally be identified as [50–53]

$$Q[\mathbf{R}_t, \omega_t] \equiv \text{tr}[H_t \dot{\rho}_t]. \quad (4)$$

Here,  $H_t \equiv H[\omega_t]$  denotes the Hamiltonian of the working system and  $\rho_t \equiv \rho[\mathbf{R}_t]$  the density matrix describing its state. Remarkably, our two-stroke scheme enables a general optimization procedure even without such specifications, as we will show in the following.

## B. Maximum Heat Extraction

Our first aim is to find the control protocol  $\omega_t^p$  that maximizes the heat extraction (2) for a given cycle time  $\tau$ . To this end we proceed along the three steps illustrated in Fig. 2.

First, for the optimal work stroke,  $\omega_t$  has to be chosen such that the extended objective functional for the extracted heat

$$\mathcal{Q}_c[\mathbf{R}_t, \boldsymbol{\lambda}_t, \omega_t] \equiv \int_0^{\tau'} (Q[\mathbf{R}_t, \omega_t] - \boldsymbol{\lambda}_t \cdot (\dot{\mathbf{R}}_t - \mathbf{F}[\mathbf{R}_t, \omega_t])) dt \quad (5)$$

becomes stationary, i.e., its functional derivative with respect to its arguments vanishes [42]. Here, we have introduced a vector of Lagrange multipliers  $\boldsymbol{\lambda}_t$  to account for the dynamical constraint (1). This extension of the parameter space makes it possible to treat the control parameter  $\omega_t$  and the state  $\mathbf{R}_t$  as independent variables. Optimizing the functional (5) is formally equivalent to applying the least-action principle in Hamiltonian mechanics with  $\mathbf{R}_t$  and  $\boldsymbol{\lambda}_t$  playing the role of generalized coordinates and canonical momenta, respectively [54]. The

corresponding effective Hamiltonian is given by

$$H_w[\mathbf{R}_t, \boldsymbol{\lambda}_t, \omega_t] \equiv Q[\mathbf{R}_t, \omega_t] + \boldsymbol{\lambda}_t \cdot \mathbf{F}[\mathbf{R}_t, \omega_t]. \quad (6)$$

Thus, after fixing the initial conditions  $\mathbf{R}_{t=0} = \mathbf{R}_0$  and  $\boldsymbol{\lambda}_{t=0} = \boldsymbol{\lambda}_0$ , the optimal protocol for the work stroke is uniquely determined by the canonical equations [42]

$$\dot{\mathbf{R}}_t = \frac{\partial H_w}{\partial \boldsymbol{\lambda}_t}, \quad \dot{\boldsymbol{\lambda}}_t = -\frac{\partial H_w}{\partial \mathbf{R}_t} \quad \text{and} \quad \frac{\partial H_w}{\partial \omega_t} = 0. \quad (7)$$

Note that the last equation is purely algebraic. Therefore, the initial value of the control parameter,  $\omega_0$ , is fixed by choosing  $\mathbf{R}_0$  and  $\boldsymbol{\lambda}_0$ .

Second, since only the work stroke contributes to the extracted heat, the optimal reset stroke minimizes the reset time  $\mathcal{T}_r \equiv \tau - \tau'$ , during which the system returns to its initial state. To implement this condition, we have to minimize the extended objective functional for the reset time

$$\begin{aligned} \mathcal{T}_r[\mathbf{R}_t, \boldsymbol{\lambda}_t, \omega_t] &\equiv \int_{\tau'}^{\tau} (1 - \boldsymbol{\lambda}_t \cdot (\dot{\mathbf{R}}_t - \mathbf{F}[\mathbf{R}_t, \omega_t])) dt \\ &\equiv \int_{\tau'}^{\tau} (H_r[\mathbf{R}_t, \boldsymbol{\lambda}_t, \omega_t] - \boldsymbol{\lambda}_t \cdot \dot{\mathbf{R}}_t) dt \end{aligned} \quad (8)$$

with respect to the dynamical variables  $\mathbf{R}_t$ ,  $\boldsymbol{\lambda}_t$  and  $\omega_t$ , and the switching time  $\tau'$ . Thus, the optimal reset protocol can be found by solving the canonical equations

$$\dot{\mathbf{R}}_t = \frac{\partial H_r}{\partial \boldsymbol{\lambda}_t}, \quad \dot{\boldsymbol{\lambda}}_t = -\frac{\partial H_r}{\partial \mathbf{R}_t} \quad \text{and} \quad \frac{\partial H_r}{\partial \omega_t} = 0 \quad (9)$$

with respect to the boundary conditions

$$\begin{aligned} \mathbf{R}_{t=\tau'} &= \mathbf{R}'[\mathbf{R}_0, \boldsymbol{\lambda}_0], \quad \mathbf{R}_{t=\tau} = \mathbf{R}_0 \quad \text{and} \\ H_r[\mathbf{R}_{\tau'}, \boldsymbol{\lambda}_{\tau'}, \omega_{\tau'}] &= 0. \end{aligned} \quad (10)$$

Here,  $\mathbf{R}'$  is the state vector of the system after the optimal work stroke, and the end-point condition  $\mathbf{R}_{t=\tau} = \mathbf{R}_0$  replaces the initial condition for the Lagrange multipliers.

Note that the state  $\mathbf{R}_t$  has to be continuous throughout the cycle [29], while the Lagrange multipliers  $\boldsymbol{\lambda}_t$  of the work and reset strokes are independent variables; they therefore do not have to satisfy any boundary conditions. The last requirement in (10) minimizes  $\mathcal{T}_r$  with respect to the initial time  $\tau'$  [42]. In practice, the switching time  $\tau'$  and the initial Lagrange multipliers  $\boldsymbol{\lambda}_{\tau'}$  have to be determined together such that the conditions (10) are satisfied.

The procedure above leads to the optimal protocol if the algebraic condition  $\partial_{\omega_t} H_r = 0$  can be satisfied throughout the reset stroke. However, the reset Hamiltonian  $H_r$  does often not have a local extremum within the admissible range  $[\omega', \omega_{\max}]$  of the control parameter [40, 44]. The optimal reset protocol  $\omega_t^p$  then has to assume one of the boundary values  $\omega'$  or  $\omega_{\max}$ , so that it minimizes the effective Hamiltonian  $H_r$ . Formally, we thus replace the last equation in (9) by the more general requirement

$$H_r[\mathbf{R}_t^p, \boldsymbol{\lambda}_t^p, \omega_t^p] \leq H_r[\mathbf{R}_t^p, \boldsymbol{\lambda}_t^p, \omega], \quad (11)$$

which is also known as Pontryagin's minimum principle [42, 46]. Here,  $\mathbf{R}_t^p$  and  $\boldsymbol{\lambda}_t^p$  are the optimal trajectories of the state vector and the Lagrange multiplier, respectively. The canonical equations (9) can thus be integrated as follows. First, for given initial conditions  $\mathbf{R}_0$  and  $\boldsymbol{\lambda}_0$ , the initial value of the control parameter,  $\omega_0$ , has to be determined such that  $H_r[\mathbf{R}_0, \boldsymbol{\lambda}_0, \omega_0]$  becomes minimal. If this function does not have a local minimum within the range  $[\omega', \omega_{\max}]$ , we either have  $\omega_0 = \omega'$  or  $\omega_0 = \omega_{\max}$ . After fixing  $\omega_0$ , the state vector and the Lagrange multipliers can be propagated for a short time  $dt$  using the canonical equations. The control parameter is then updated by minimizing the Hamiltonian  $H_r[\mathbf{R}_{dt}, \boldsymbol{\lambda}_{dt}, \omega_{dt}]$  with respect to  $\omega_{dt}$ . Iterating this procedure until the final time  $\tau$  yields the optimal trajectories  $\mathbf{R}_t^p$ ,  $\boldsymbol{\lambda}_t^p$  and  $\omega_t^p$ . This prescription typically leads to protocols that are either constant or consist of constant pieces connected by continuous trajectories [43]. In Sec. III, we will show how both of these cases can be handled in practice.

Third and finally, after completing steps 1 and 2, we arrive at the optimal protocol  $\omega_t^p = \omega_t^p[\mathbf{R}_0, \boldsymbol{\lambda}_0]$  for fixed initial conditions  $\mathbf{R}_0$  and  $\boldsymbol{\lambda}_0$ . Inserting this solution into (2) renders the extracted heat an ordinary function of  $2N$  variables,  $Q_c = Q_c[\mathbf{R}_0, \boldsymbol{\lambda}_0]$ . The last step of our scheme thus consists of maximizing this function over the state space of the working system and the set of admissible Lagrange multipliers, i.e., those  $\boldsymbol{\lambda}_0$ , for which  $\omega_0 = \omega_0[\mathbf{R}_0, \boldsymbol{\lambda}_0]$  falls into the permitted range  $[\omega_{\min}, \omega']$ . We note that maximizing  $Q_c$  over all initial conditions  $\mathbf{R}_0$  and  $\boldsymbol{\lambda}_0$  is equivalent to maximizing  $Q_c$  over all switching times  $\tau'$  and all boundary values  $\mathbf{R}_0$  and  $\mathbf{R}'$ , since these quantities are connected by a one-to-one mapping.

### C. Maximum Efficiency

So far, we have developed a scheme to maximize the extracted heat per operation cycle of a general two-stroke refrigerator. A thorough optimization of a thermal machine, however, also has to take into account the consumed input, which, for a cooling device, corresponds to the work  $\mathcal{W}[\omega_t]$  that the external controller has to supply to drive the heat flux. To this end, we now show how to find the optimal protocol  $\omega_t^\eta$ , which maximizes the efficiency

$$\begin{aligned} \eta[\omega_t] &\equiv Q_c[\omega_t]/\mathcal{W}[\omega_t] \\ &= Q_c[\omega_t]/(Q_h[\omega_t] - Q_c[\omega_t]), \end{aligned} \quad (12)$$

a second key indicator for thermodynamic performance [47]. Note that here we have used the first law of thermodynamics to express the work input  $\mathcal{W}[\omega_t]$  in terms of the released and the extracted heat,  $Q_h[\omega_t]$  and  $Q_c[\omega_t]$ . Owing to the second law, the figure of merit (12) is subject to the Carnot bound

$$\eta[\omega_t] \leq \eta_C \equiv \frac{T_c}{T_h - T_c}, \quad (13)$$

which is saturated in the reversible limit at the price of vanishing cooling power [17]. Hence, for a practical optimization criterion, we have to fix both the cycle time  $\tau$  and the heat extraction  $Q_c[\omega_t] = Q_c^*$ . Maximizing the efficiency (12) then amounts to minimizing the effective input  $Q_h[\omega_t]$ , i.e., the average heat injected into the hot reservoir per operation cycle.

The corresponding protocol  $\omega_t^\eta = \omega_t^\eta[Q_c^*]$  renders the work stroke as short as possible such that the maximum amount of time is left to reduce the heat release in the reset stroke [55]. Hence, in the first step, we have to minimize the working time

$$\begin{aligned} \mathcal{T}_w[\mathbf{R}_t, \boldsymbol{\lambda}_t, \omega_t, \mu] \\ \equiv \int_0^{\tau'} (1 - \mu(Q_c^* + \boldsymbol{\lambda}_t \cdot \dot{\mathbf{R}}_t - H_w[\mathbf{R}_t, \boldsymbol{\lambda}_t, \omega_t])) dt, \end{aligned} \quad (14)$$

where the time-independent Lagrange multiplier  $\mu$  has been introduced to fix the total heat extraction  $Q_c^*$ . This variational problem again leads to the canonical equations (7), which have to be solved for given initial conditions  $\mathbf{R}_0$  and  $\boldsymbol{\lambda}_0$  to find the optimal work protocol. In fact, this protocol also maximizes the heat extraction for every given time  $t$ , i.e., we have  $\omega_t^\eta[\mathbf{R}_0, \boldsymbol{\lambda}_0] = \omega_t^p[\mathbf{R}_0, \boldsymbol{\lambda}_0]$  during the work stroke. However, the switching time  $\tau' = \tau'[\mathbf{R}_0, \boldsymbol{\lambda}_0, Q_c^*]$  now has to be chosen such that the constraint

$$\int_0^{\tau'} Q[\mathbf{R}_t, \omega_t] dt = Q_c^* \quad (15)$$

is satisfied. Hence, the switching time is now determined by the work stroke rather than the reset stroke.

After completing step 1, the optimal reset protocol is found by minimizing the functional

$$\mathcal{Q}_h[\mathbf{R}_t, \boldsymbol{\lambda}_t, \omega_t] \equiv \int_{\tau'}^{\tau} (-Q[\mathbf{R}_t, \omega_t] - \boldsymbol{\lambda}_t \cdot (\dot{\mathbf{R}}_t - \mathbf{F}[\mathbf{R}_t, \omega_t])) dt \quad (16)$$

for the boundary conditions

$$\mathbf{R}_{t=\tau'} = \mathbf{R}'[\mathbf{R}_0, \boldsymbol{\lambda}_0, \mathcal{Q}_c^*] \quad \text{and} \quad \mathbf{R}_{t=\tau} = \mathbf{R}_0. \quad (17)$$

This problem will, depending on the initial conditions, only admit a proper solution if the device can actually produce the cooling power  $\mathcal{Q}_c^*/\tau$  in a cyclic mode of operation. It might therefore be helpful to introduce an intermediate step, which decides whether or not the cycle can be closed for the boundary conditions (17). To solve the canonical equations for the objective functional (16), it might again be necessary to invoke Pontryagin's minimum principle, as we will demonstrate explicitly in Sec. III D.

Once the reset protocol has been determined, the efficiency (12) can be reduced to an ordinary function of  $\mathbf{R}_0$  and  $\boldsymbol{\lambda}_0$ . Maximizing this function under the constraint  $\omega_0[\mathbf{R}_0, \boldsymbol{\lambda}_0] \in [\omega_{\min}, \omega']$  yields the maximal-efficiency protocol  $\omega_t^n[\mathcal{Q}_c^*]$ . Note that the set of admissible initial conditions is thereby also restricted by fixing the heat extraction  $\mathcal{Q}_c^*$ .

### III. QUANTUM MICROCOOLER I – SEMICLASSICAL REGIME

#### A. System

We will now show how our general theory can be applied to a concrete problem of quantum engineering. Specifically, we optimize the performance of a quantum microcooler, which can be implemented with superconducting components, see Fig. 3a. The core of this device is an engineered two-level system with Hamiltonian [17]

$$H_t \equiv \frac{\hbar\Delta}{2}\sigma_x + \frac{\hbar\omega_t}{2}\sigma_z. \quad (18)$$

Here,  $\hbar$  denotes the reduced Planck constant,  $\sigma_x$  and  $\sigma_z$  are Pauli matrices,  $\Delta$  corresponds to the device-specific tunneling energy and  $\omega_t$  is the tunable energy bias, which plays the role of the external control parameter. This system is embedded in an electronic circuit, which couples it either to a cold or a hot reservoir depending on the value of  $\omega_t$ . Thus, applying a suitable periodic control protocol  $\omega_t$  makes it possible to realize a two-stroke cooling cycle, as illustrated in Fig. 3b.

#### B. Step-Rate Model

For a quantitative description of the microcooler, we consider the model shown in Fig. 3a, which makes it

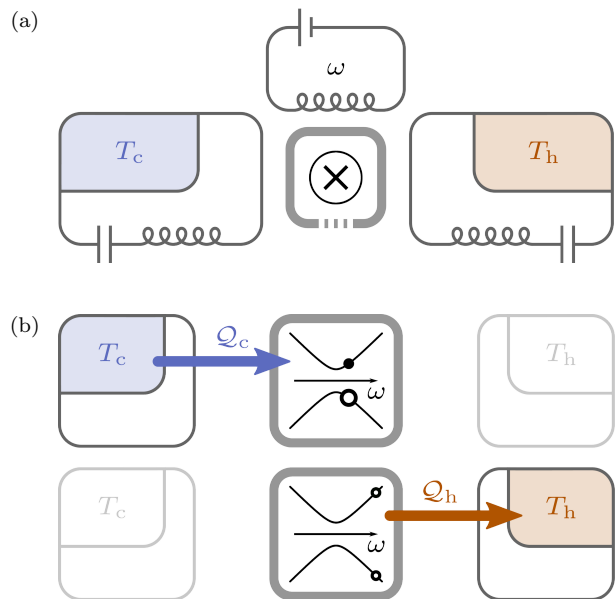


Figure 3. Quantum microcooler. (a) Sketch of the experimental setup described in Refs. [15, 17, 38]. A superconducting qubit is coupled to two resonant circuits with different resonance frequencies. Each circuit contains a metallic island acting as a mesoscopic reservoir with temperature  $T_c$  and  $T_h > T_c$ , respectively. An additional bias circuit is used to control the level splitting of the qubit by varying the applied magnetic flux. (b) Scheme of the thermodynamic cooling cycle. The two central diagrams show the energy levels of the qubit as a function of the external bias  $\omega$  and the corresponding populations at the beginning of each stroke. By the end of the work stroke, the qubit has picked up the heat  $\mathcal{Q}_c$  from the cold island. The level splitting is then instantaneously increased to tune the qubit into resonance with the hot island. During the following reset stroke, the initial level populations are restored, while the heat  $\mathcal{Q}_h$  flows into the hot reservoir. The cycle is completed by setting the level splitting back to its initial value, thus reconnecting the qubit to the cold island.

possible to determine the optimal control protocol analytically. To this end, we here focus on the semiclassical limit, where the tunneling energy  $\Delta$  is negligible and the Hamiltonian commutes with itself at different times. The periodic density matrix of the working system is then fully determined by the level populations and can be parametrized as

$$\rho_t \equiv \frac{1}{2}(\mathbb{1} + R_t \sigma_z). \quad (19)$$

The state variable  $R_t$  thereby obeys the Bloch equation [52]

$$\dot{R}_t = F[R_t, \omega_t] \equiv -\Gamma^+[\omega_t] R_t - \Gamma^-[\omega_t] \quad \text{with} \quad (20)$$

$$\Gamma^\pm[\omega_t] \equiv \gamma[\omega_t](1 \pm \exp[-\hbar\omega_t/T[\omega_t]]).$$

Here, the Boltzmann factors appear due to the detailed balance condition, which fixes the relative frequency of thermal excitation and relaxation events [47]. The corresponding temperature is determined by the reservoir

coupled to the system, i.e.,

$$T[\omega \leq \omega'] \equiv T_c \quad \text{and} \quad T[\omega > \omega'] \equiv T_h, \quad (21)$$

where  $\omega'$  corresponds to the threshold energy of the device. Note that Boltzmann's constant is set to 1 throughout. The factor  $\gamma[\omega]$  in (20) accounts for the finite energy range of the coupling mechanism between working system and reservoirs, which depends on the specific design of the circuit. For the sake of simplicity, we here use an idealized model, where the rates (20) feature a step-type dependence on  $\omega$ , i.e., we set

$$\gamma[\omega] \equiv \gamma = \text{const. for } 0 < \omega \leq \omega_{\max} \quad (22)$$

and  $\gamma[\omega] \equiv 0$  otherwise. Hence, the two-level system is decoupled from its environment if  $\omega$  falls outside its admissible range. Note that we have set  $\omega_{\min}$  to zero.

Under weak-coupling conditions, the instantaneous heat flux into the qubit is given by (4). The average amount of heat that the microcooler extracts from the cold reservoir in one cycle of duration  $\tau$  then becomes

$$\mathcal{Q}_c[\omega_t] \equiv \int_0^{\tau'} \frac{\hbar\omega_t}{2} \dot{R}_t dt = \int_0^{\tau'} \frac{\hbar\omega_t}{2} F[R_t, \omega_t] dt, \quad (23)$$

where  $\tau' \in [0, \tau]$  denotes the length of the work stroke. Accordingly, the average heat injected into the hot reservoir is given by

$$\mathcal{Q}_h[\omega_t] \equiv - \int_{\tau'}^{\tau} \frac{\hbar\omega_t}{2} F[R_t, \omega_t] dt. \quad (24)$$

### C. Maximum Heat Extraction

The extracted heat (23) can be maximized using the general scheme of Sec. II B. To this end, we first have to determine the optimal work stroke, which is described by the effective Hamiltonian [56]

$$H_w[R_t, \lambda_t, \omega_t] = -(\omega_t + \lambda_t)(\Gamma^+[\omega_t]R_t + \Gamma^-[\omega_t]). \quad (25)$$

The corresponding canonical equations follow from (7) and are given by

$$\begin{aligned} \dot{R}_t &= -\Gamma^+[\omega_t]R_t - \Gamma^-[\omega_t], \\ \dot{\lambda}_t &= \Gamma^+[\omega_t](\omega_t + \lambda_t) \quad \text{and} \\ \omega_t &= (T_c/\hbar) - \lambda_t - (T_c/\hbar)W_0 \left[ e^{1-\hbar\lambda_t/T_c} \frac{1+R_t}{1-R_t} \right], \end{aligned} \quad (26)$$

where we have explicitly solved the last equation for  $\omega_t$ . We used that  $\gamma[\omega_t] = \gamma$  and  $T[\omega_t] = T_c$  throughout the work stroke and  $W_0$  denotes the upper branch of the Lambert  $W$  function, which is defined as the solution to

$$x \equiv W[x]e^{W[x]} \quad \text{for } x \geq -1/e. \quad (27)$$

Upon eliminating  $\omega_t$ , the canonical equations (26) reduce to an autonomous system of first-order differential equations,

$$\begin{pmatrix} \dot{R}_t \\ \dot{\lambda}_t \end{pmatrix} = \begin{pmatrix} \Phi_R[R_t, \lambda_t] \\ \Phi_\lambda[R_t, \lambda_t] \end{pmatrix} \equiv \Phi[R_t, \lambda_t] \quad (28)$$

The flow of the Hamiltonian vector field  $\Phi[R, \lambda]$  is plotted in Fig. 4a. As a key observation, we find that the sign of  $\dot{R}_t = \Phi_R[R_t, \lambda_t]$ , which determines the direction of the instantaneous heat flux  $Q_t = \hbar\omega_t \dot{R}_t/2$ , does not change along the optimal trajectories. Hence, since our aim is to maximize the heat extraction from the cold reservoir, the initial values  $R_0$  and  $\lambda_0$  have to be chosen such that

$$\dot{R}_0 = \Phi_R[R_0, \lambda_0] > 0. \quad (29)$$

Solving (28) under this condition and inserting the result into the third canonical equation (26) yields the protocol

$$\omega_t^p = \frac{T_c}{\hbar} \ln \left[ \frac{2 - 2C_1 W_{-1}[C_2 e^{-\gamma t}]}{C_1 W_{-1}[C_2 e^{-\gamma t}]^2} - 1 \right] \quad (30)$$

and the corresponding state trajectory

$$R_t^p = C_1 (1 + W_{-1}[C_2 e^{-\gamma t}])^2 - C_1 - 1. \quad (31)$$

Here,  $W_{-1}$  denotes the lower branch of the Lambert  $W$  function and the constants  $C_1$  and  $C_2$  can be expressed in terms of the initial values  $R_0$  and  $\omega_0$ , see Appendix A. We note that the results (30) and (31) can also be obtained using a brute-force approach, where the dynamical constraint (20) is solved explicitly rather than being enforced through a Lagrange multiplier. (For further details see Appendix A.) However, this approach crucially relies on the one-to-one correspondence (20) between the derivative  $\dot{R}_t$  of the state variable and the control parameter  $\omega_t$ . It is therefore not generally applicable.

To close the optimal cycle, the reset stroke has to restore the initial state  $R_0$  of the system in minimal time. According to Pontryagin's principle, the corresponding protocol can be found by minimizing the effective Hamiltonian

$$H_r[R_t, \lambda_t, \omega_t] = 1 + \lambda_t F[R_t, \omega_t] \quad (32)$$

with respect to  $\omega_t$ . The variables  $R_t$  and  $\lambda_t$  thereby have to obey the canonical equations

$$\dot{R}_t = F[R_t, \omega_t] \quad \text{and} \quad \dot{\lambda}_t = \Gamma^+[\omega_t] \lambda_t \quad (33)$$

and the additional constraint

$$H_r[R_{\tau'}, \lambda_{\tau'}, \omega_{\tau'}] = 0 \quad (34)$$

at the yet undetermined optimal switching time  $\tau'$ .

This problem can be approached as follows. First, we observe that (34) implies

$$\lambda_{\tau'} = -1/F[R_{\tau'}, \omega_{\tau'}] = -1/\dot{R}_{\tau'}. \quad (35)$$



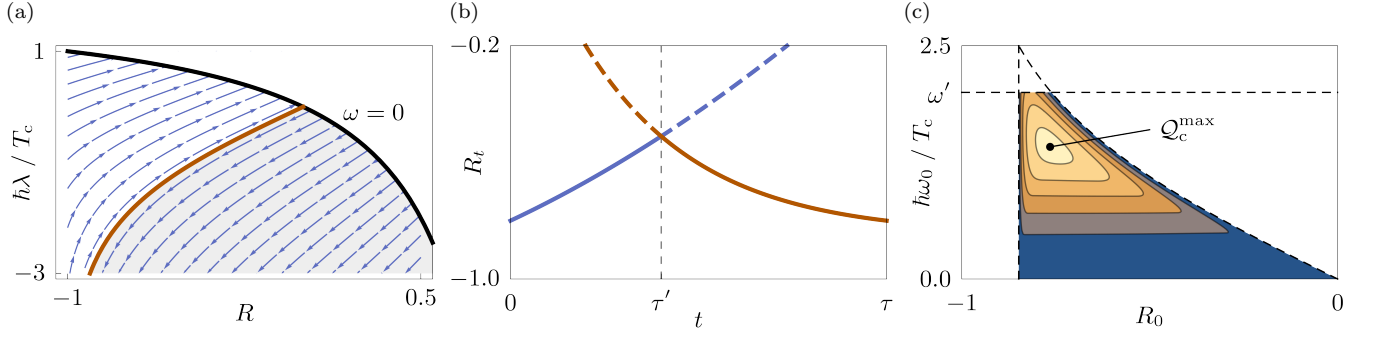


Figure 4. Maximizing the cooling power of a quantum microcooler in three steps. (a) The plot shows the flow of the effective Hamiltonian vector field (28), which determines the optimal dynamics of the system during the work stroke. The black line marks the boundary of the physical region of the effective phase space, where the level splitting  $\omega$  is positive. The red line separates solutions with positive (unshaded) and negative (shaded) cooling power. (b) The state trajectories during the optimal work and reset stroke, (31) and (36), are plotted in blue and red, respectively, for typical initial conditions. Their intersection point determines the optimal switching time  $\tau'$ . The solid line shows the combined optimal state trajectory, which excludes the dashed parts. (c) The maximum heat extraction  $\mathcal{Q}_c[R_0, \omega_0]$  is plotted over the admissible range (37) of initial conditions, which is bounded by the dashed black curves corresponding to  $R_0 = -\tanh[\hbar\omega_0/(2T_c)]$ ,  $R_0 = -\tanh[\hbar\omega_{\max}/(2T_h)]$  and  $\omega_0 = \omega'$ . Brighter colors indicate a larger amount of extracted heat. The global maximum  $\mathcal{Q}_c^{\max}$  is shown with a dot. All panels were created with the parameter values  $\omega' = 2T_c/\hbar$ ,  $\omega_{\max} = 5T_c/\hbar$ ,  $T_h = 2T_c$  and  $\tau = 3/\gamma$ .

Since  $R_t$  increases monotonically during the work stroke, it has to decrease during the reset. Consequently, we have to choose  $\lambda_{\tau'} > 0$ . Minimizing the effective Hamiltonian (32) at the switching time  $\tau'$  is then equivalent to minimizing  $F[R_{\tau'}, \omega_{\tau'}]$ . Second, the generator  $F$  is a monotonically decreasing function of  $\omega_{\tau'}$  for any admissible value of  $R_{\tau'}$ . Thus, it follows that  $\omega_{\tau'} = \omega_{\max}$ , i.e., the control parameter abruptly jumps to its maximum at the beginning of the reset stroke. Third, owing to (33), the sign of the Lagrange multiplier is conserved along its optimal trajectory. Therefore, the same argument applies at any later time  $t > \tau'$  and we can conclude that  $\omega_t^p = \omega_{\max}$  throughout the reset stroke. We note that this result could have been inferred directly from the Bloch equation (20) and the observation  $\partial_{\omega_t} F[R_t, \omega_t] < 0$ , which entails that the reset can always be accelerated by increasing  $\omega_t$ . However, here we have chosen to follow the formal scheme of Sec. II to illustrate the use of Pontryagin's principle.

Finally, we have to make sure that the state  $R_t$  is continuous throughout the cycle. To this end, its trajectory during the reset stroke,

$$R_t^p = R_0 e^{\Gamma^+(\tau-t)} + (\Gamma^-/\Gamma^+) \left( e^{\Gamma^+(\tau-t)} - 1 \right) \quad (36)$$

with  $\Gamma^\pm \equiv \Gamma^\pm[\omega_{\max}]$ , has to match the optimal work-stroke trajectory (31) at  $\tau'$ , see Fig. 4b. Numerically solving this condition yields the switching time  $\tau'$  and completes the optimal protocol  $\omega_t^p[R_0, \omega_0]$  [57]. Inserting this protocol back into the functional (23) together with (31) and (36) gives the maximal heat extraction  $\mathcal{Q}_c[R_0, \omega_0]$ .

This function must now be maximized over the admissible range of initial values  $R_0$  and  $\omega_0$ , which is restricted

by the conditions

$$\begin{aligned} R_0 &< -\tanh[\hbar\omega_0/(2T_c)], \\ R_0 &> -\tanh[\hbar\omega_{\max}/(2T_h)] \end{aligned} \quad (37)$$

and the requirement that  $\omega_0 \leq \omega'$ , see Fig. 4c. The constraints (37) follow from (29) and (36), respectively. They ensure that the heat extraction  $\mathcal{Q}_c[R_0, \omega_0]$  is positive and that the initial state of the system can be restored during the reset. To determine the maximal extracted heat  $\mathcal{Q}_c^{\max}$  and the corresponding initial values, we employ a constrained optimization algorithm [58], which finds  $\mathcal{Q}_c^{\max}$  either inside the admissible range (37) or on the boundary  $\omega_0 = \omega'$ .

Figure 5a summarizes the results of this section. The first plot shows the optimal cooling power  $\mathcal{Q}_c^{\max}/\tau$  as a function of the cycle time  $\tau$  for different values of the high temperature  $T_h$ . We find that  $\mathcal{Q}_c^{\max}/\tau$  generally decreases with  $\tau$ . Hence, for a large cooling power, the device must be operated fast. For similar recent findings, the reader may consult Refs. [27, 41]. Furthermore, the cooling power becomes successively smaller as  $T_h$  increases. This result confirms the natural expectation that the microcooler becomes less effective when it has to work against a larger temperature gradient.

Figure 5b illustrates the general behavior of our model during the optimal cycle. In the work stroke, the state variable  $R_t^p$  monotonically increases, while the control parameter  $\omega_t^p$  monotonically decreases until the switching time is reached; at this point, no more heat can be extracted from the cold reservoir in a cyclic mode of operation, i.e., the work stroke has reached the maximal length. In the reset stroke, the control parameter is constantly at its maximum, while  $R_t$  returns to its initial value following an exponential decay.

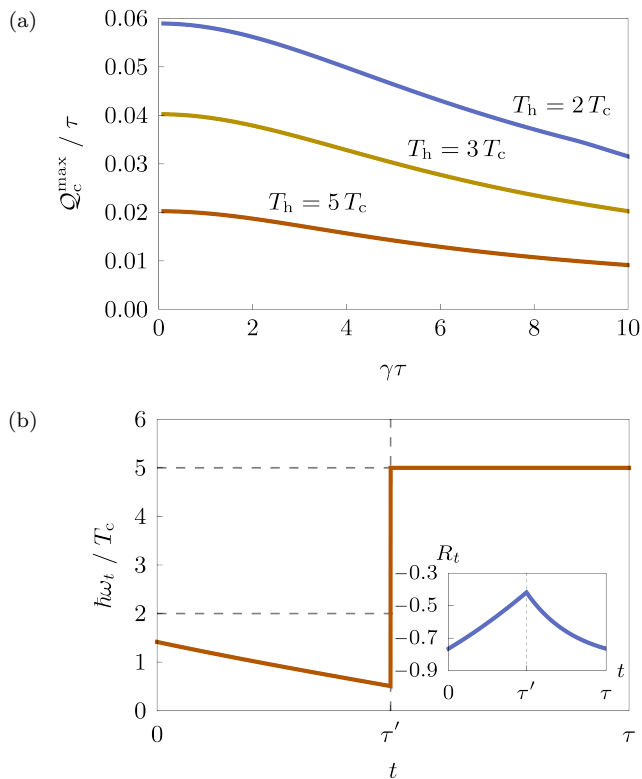


Figure 5. Microcooler at optimal cooling power. (a) Maximum cooling power in units of  $\gamma T_c$  as a function of the dimensionless cycle time  $\gamma\tau$  for different temperatures of the hot reservoir  $T_h$ . (b) Optimal control protocol for  $T_h = 2 T_c$  and  $\tau = 2 \gamma^{-1}$ . The inset shows the corresponding trajectory of the state variable  $R_t$ . Here, we have used  $\omega' = 2 T_c / \hbar$  and  $\omega_{\max} = 5 T_c / \hbar$ .

#### D. Maximum Efficiency

Having maximized the extracted heat of our microcooler model, we now focus on its thermodynamic efficiency (12). The optimal protocol  $\omega_t^\eta[Q_c^*]$ , which maximizes this figure of merit for a fixed heat extraction  $Q_c^*$ , can be found using the scheme developed in Sec. II C. During the work stroke, we have  $\omega_t^\eta[R_0, \omega_0] = \omega_t^p[R_0, \omega_0]$ , that is, for  $0 \leq t \leq \tau'$  and fixed initial values  $R_0$  and  $\omega_0$ , the protocol  $\omega_t^\eta[Q_c^*]$  is given by (30). The switching time  $\tau'$  can thus be determined from the constraint

$$\int_0^{\tau'} \frac{\hbar\omega_t}{2} F[R_t, \omega_t] dt = Q_c^* \quad (38)$$

using (30) and (31).

The optimal reset stroke has to restore the initial state of the system while at the same time minimizing the dissipated heat  $Q_h[\omega_t]$ . To this end, the control protocol has to be chosen such that the effective Hamiltonian

$$H_r[R_t, \lambda_t, \omega_t] = (\omega_t + \lambda_t)(\Gamma^+[R_t] + \Gamma^-[R_t]) \quad (39)$$

becomes minimal at every time  $\tau' \leq t \leq \tau$ , while  $\lambda_t$  and  $R_t$  obey the corresponding canonical equations. For

a given initial value  $\lambda_0$  of the Lagrange multiplier, this problem can be solved using the procedure described in Sec. II C. However, the situation is in practice complicated by the fact that  $\lambda_0$  is determined only implicitly by the end-point condition  $R_\tau = R_0$ . It would still be possible to carry out the iteration scheme for every admissible value  $\lambda_0$  and then pick the optimal protocol that closes the cycle. This approach can, however, be expected to be numerically costly and hard to implement with sufficient accuracy.

In the following, we describe a more practical way of finding the optimal reset protocol. To this end, we first note that the Hamiltonian (39) is, up to its sign, identical with (25). Thus, if  $H_r$  admits a local minimum with respect to  $\omega_t$  in the range  $[\omega', \omega_{\max}]$ , the canonical equations can be solved exactly and the reset protocol reads

$$\omega_t = \frac{T_c}{\hbar} \ln \left[ \frac{2 - 2C_1 W_0 [C_2 e^{-\gamma t}]}{C_1 W_0 [C_2 e^{-\gamma t}]^2} - 1 \right], \quad (40)$$

where  $C_1$  and  $C_2$  are constants. Note that, in contrast to (30), this solution must involve the upper rather than the lower branch of the Lambert  $W$  function to ensure that the state variable decreases during the reset, i.e.,  $\dot{R}_t = F[R_t, \omega_t] < 0$ . According to Pontryagin's principle, the protocol  $\omega_t^\eta$  either follows the monotonically increasing trajectory (40) or takes on one of the boundary values  $\omega'$  or  $\omega_{\max}$ . Consequently, if we assume that the optimal protocol does not jump within the reset stroke, it must have the general form shown in Fig. 6b. Specifically,  $\omega_t^\eta$  must be constant at  $\omega'$  until a certain time  $\tau_1$ , then follow (40) until it reaches  $\omega_{\max}$ , and finally remain constant until the end of the stroke. Since each protocol of this type is uniquely determined by the departure time  $\tau_1$  and the state of the system at the end of the reset stroke,  $R_\tau = R_\tau[\tau_1]$ . This map can be determined analytically from the corresponding Bloch equation. The only numerical operation that is required to determine the optimal reset protocol thus consists in solving the condition  $R_\tau[\tau_1] = R_0$  for  $\tau_1$  [59].

The method described above makes it possible to find the protocol  $\omega_t^\eta[R_0, \omega_0, Q_c^*]$  that maximizes the efficiency of the cooling cycle for given  $R_0$ ,  $\omega_0$  and  $Q_c^*$ . Inserting this protocol into (12) and optimizing the resulting function  $\eta[R_0, \omega_0, Q_c^*]$  with respect to the initial values  $R_0$  and  $\omega_0$  finally yields the maximal efficiency at given cooling power.

This figure of merit is plotted in Fig. 6 together with the corresponding optimal protocol; it approaches the Carnot limit (13) for  $Q_c^* \rightarrow 0$  and monotonically decays as  $Q_c^*$  becomes larger. Thus, increasing the heat extraction of the microcooler inevitably reduces its maximal efficiency. This result aligns well with recent discoveries of universal trade-off relations between the extracted heat and the efficiency of mesoscopic thermal devices [33, 34, 37, 60–62]. Furthermore, Fig. 6a shows that not only the maximal cooling power but also the overall ef-



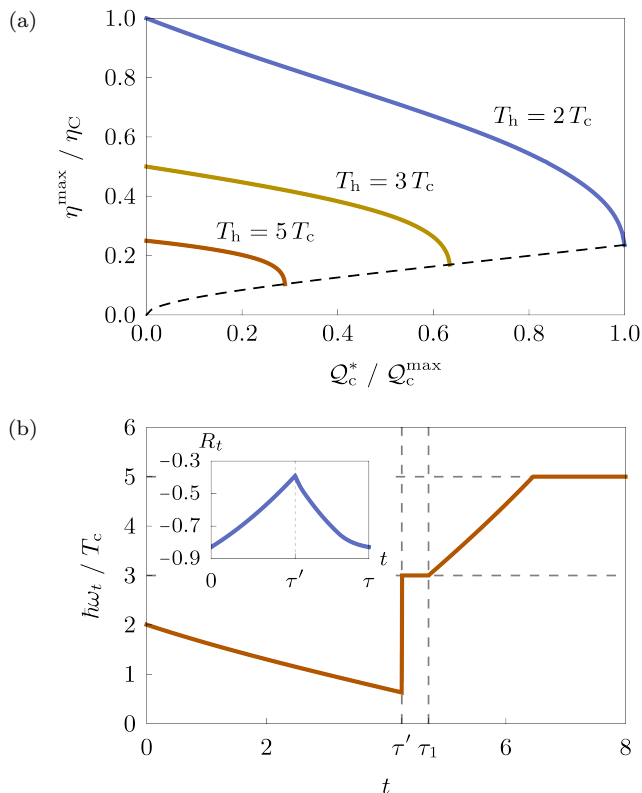


Figure 6. Microcooler at optimal efficiency. (a) Maximum efficiency as a function of the given heat extraction  $Q_c^*$ . The horizontal axis has been rescaled with the maximum heat extraction for  $T_h = 2T_c$ ,  $Q_c^{\max}$ , and the vertical axis with the Carnot efficiency  $\eta_C$  for the same temperatures. The dashed line shows how the efficiency at maximal cooling power decays as the temperature gradient becomes larger. (b) Optimal control protocol leading to maximal efficiency for fixed heat extraction  $Q_c^* = 0.9 Q_c^{\max}$ . The inset shows the corresponding trajectory of the state variable  $R_t$ . Throughout this figure, we have set  $\omega' = 3T_c/\hbar$ ,  $\omega_{\max} = 5T_c/\hbar$ ,  $T_h = 2T_h$  and  $\tau = 8\gamma^{-1}$ . For these parameter values, the maximum extracted heat at  $T_h = 2T_c$  is  $Q_c^{\max} \approx 0.297 T_c$ .

efficiency decays as the temperature of the hot reservoir becomes larger. Hence, increasing the temperature bias is generally detrimental to the performance of the microcooler.

## IV. APPROXIMATION METHODS

### A. Rationale

Our two-stroke scheme makes it possible to systematically optimize realistic models for mesoscopic thermal machines, as we have shown in the previous section for a superconducting microcooler. To explore the optimal performance of even more complex devices, it is often helpful to first focus on limiting regimes, where dynamical approximation methods can be used to simplify computational tasks. In this section, we develop such

schemes for the key limits of slow or fast driving. We thereby further extend our general framework and prepare the stage to investigate the thermodynamic performance of mesoscopic refrigerators in the coherent regime.

### B. Adiabatic Response

We consider a slowly operated two-stroke refrigerator by assuming  $\tau, \tau' \gg 1/\gamma$ , where  $\gamma$  is the typical relaxation rate of the working system. Except for short transient periods at the beginning of each stroke, the system then follows the instantaneous equilibrium state  $\mathbf{R}_{\text{eq}}[\omega_t]$ , which is defined by the condition

$$\mathbf{F}[\mathbf{R}_{\text{eq}}[\omega_t], \omega_t] \equiv 0. \quad (41)$$

In particular, we have

$$\mathbf{R}_{\tau'} \simeq \mathbf{R}_{\text{eq}}[\omega_w] \quad \text{and} \quad \mathbf{R}_\tau \simeq \mathbf{R}_{\text{eq}}[\omega_r], \quad (42)$$

where  $\omega_w$  and  $\omega_r$  are the values of the control parameter at the end of the work and the reset stroke, respectively. We note that this approximation can be systematically refined by including finite-time corrections. To this end, the time-evolution equation (1) has to be solved perturbatively by expanding the state vector  $\mathbf{R}_t$  in powers of the adiabaticity parameter  $\varepsilon \equiv 1/(\gamma\tau)$  [63]. However, to keep our analysis as transparent and simple as possible, we here neglect contributions of order  $\varepsilon$ . The relations (42) significantly reduce the interdependence of work and reset stroke, and thus simplify our optimization scheme as follows.

To maximize the heat extraction (2), the work protocol has to be found by solving the canonical equations (7) for fixed initial conditions  $\mathbf{R}_0$  and  $\boldsymbol{\lambda}_0$ . Since  $\mathbf{R}_t$  does not change during the quenches of  $\omega_t$ , we now have  $\mathbf{R}_0 = \mathbf{R}_{\text{eq}}[\omega_r]$ , i.e., the initial state of the system is determined by one parameter  $\omega_r$ . Moreover, to restore this state after the work stroke, it suffices to set  $\omega_t = \omega_r$  for a short time  $\mathcal{T}_r \simeq 1/\gamma \equiv \varepsilon\tau$ . Hence, in the zeroth order with respect to  $\varepsilon$ , we have  $\tau \simeq \tau'$  and the reset stroke does not have to be optimized separately. In fact, the optimal protocol  $\omega_t^p$  is obtained by extending the work stroke over the entire cycle time  $\tau$  and maximizing the resulting heat extraction over  $N + 1$  parameters given by  $\boldsymbol{\lambda}_0$  and  $\omega_r$ .

Our second optimization criterion requires us to minimize the dissipated heat (3) for given cooling power  $Q_c^*/\tau$ . To this end, both strokes have to be taken into account. Specifically, after finding the optimal work protocol  $\omega_t[\omega_r, \boldsymbol{\lambda}_0]$  as before, we first have to determine the switching time  $\tau'[\omega_r, \boldsymbol{\lambda}_0, Q_c^*]$  such that  $Q_c[\omega_t] = Q_c^*$ , cf. (15). To find the optimal reset protocol, the objective functional (16) has to be minimized using fixed initial conditions  $\mathbf{R}_{\tau'} = \mathbf{R}_{\text{eq}}[\omega_w]$  and  $\boldsymbol{\lambda}_{\tau'}$  for the state variables and Lagrange multipliers, respectively. Here,  $\omega_w$  is determined by  $\omega_r$  and  $\boldsymbol{\lambda}_0$ ;  $\boldsymbol{\lambda}_{\tau'}$  has to be chosen such that the cycle condition  $\omega_\tau = \omega_r$  is satisfied. Owing to this constraint, the optimal protocol  $\omega_t^n[\omega_r, \boldsymbol{\lambda}_0, \boldsymbol{\lambda}_{\tau'}, Q_c^*]$  effectively depends on  $2N$  free parameters, which have to be

eliminated by minimizing the corresponding heat release  $\mathcal{Q}_h[\omega_\tau, \lambda_0, \lambda_{\tau'}]$ . Though generally non-trivial, this procedure is still significantly simpler than the full optimization, which involves  $N$  boundary conditions to ensure that  $\mathbf{R}_\tau = \mathbf{R}_0$ . By contrast, here only one constraint has to be respected. The continuity of the state  $\mathbf{R}_t$  is then enforced by the adiabaticity condition (42).

### C. High-Frequency Response

Having understood how to optimize a two-stroke refrigerator in adiabatic response, we now consider the opposite limit  $\tau, \tau' \ll 1/\gamma$ . In this regime, the state vector  $\mathbf{R}_t$  changes only slightly during the individual strokes, since the working system is unable to follow the rapid variations of the control parameter  $\omega_t$ . Therefore, we can use the approximations

$$\begin{aligned} \mathbf{R}_t &\simeq \mathbf{R}_0 + t\dot{\mathbf{R}}_0 = \mathbf{R}_0 + t\mathbf{F}[\mathbf{R}_0, \omega_0] \quad \text{and} \quad (43) \\ \mathbf{R}_t &\simeq \mathbf{R}_{\tau'} + (t - \tau')\dot{\mathbf{R}}_{\tau'} = \mathbf{R}_{\tau'} + (t - \tau')\mathbf{F}[\mathbf{R}_{\tau'}, \omega_{\tau'}] \end{aligned}$$

to describe the work and the reset stroke, respectively. The initial states  $\mathbf{R}_0$  and  $\mathbf{R}_{\tau'}$  are thereby fully determined as functions of  $\omega_0$  and  $\omega_{\tau'}$  by the requirement that  $\mathbf{R}_t$  is continuous throughout the cycle. Thus, inserting the expansions (43) into (2) and (3) and neglecting second-order corrections in  $1/\varepsilon \equiv \gamma\tau$  yields

$$\begin{aligned} \mathcal{Q}_c[\omega_t] &\simeq \tau' Q[\mathbf{R}_0, \omega_0] \equiv \mathcal{Q}_c[\tau', \omega_0, \omega_{\tau'}] \quad \text{and} \quad (44) \\ \mathcal{Q}_h[\omega_t] &\simeq (\tau' - \tau) Q[\mathbf{R}_{\tau'}, \omega_{\tau'}] \equiv \mathcal{Q}_h[\tau', \omega_0, \omega_{\tau'}]. \end{aligned}$$

These expressions show that both the extracted and the released heat of the device now depend only on the switching time  $\tau'$  and the initial values of the work and the reset protocols,  $\omega_0$  and  $\omega_{\tau'}$ . Consequently, any control protocol  $\omega_t$  can be mimicked with a step profile

$$\omega_t^{\text{HF}}[\tau', \omega_0, \omega_{\tau'}] = \omega_0 + (\omega_{\tau'} - \omega_0)\Theta[t - \tau'], \quad (45)$$

where  $\Theta$  denotes the Heaviside function. In particular, the optimal protocols  $\omega_t^{\text{P}}$  and  $\omega_t^{\text{H}}[\mathcal{Q}_c^*]$  adopt the form (45) in the fast-driving limit. For  $\omega_t^{\text{P}}$ , the free parameters  $\tau', \omega_0$  and  $\omega_{\tau'}$  must be determined by maximizing  $\mathcal{Q}_c[\tau', \omega_0, \omega_{\tau'}]$ . Analogously,  $\omega_t^{\text{H}}[\mathcal{Q}_c^*]$  is found by minimizing  $\mathcal{Q}_h[\tau', \omega_0, \omega_{\tau'}]$  under the constraint  $\mathcal{Q}_c[\tau', \omega_0, \omega_{\tau'}] = \mathcal{Q}_c^*$ .

The high-frequency approximation provides a simple yet powerful tool to explore the performance limits of mesoscopic refrigerators. In fact, due to the universal form (45) of the high-frequency protocol, our general scheme can be reduced to relatively simple 3-parameter optimizations. Moreover, the approximations (43) and (44) can be systematically refined by including higher-order corrections in  $1/\varepsilon$ , and thus introducing more and more variational parameters given by the higher derivatives of  $\omega_t$  at  $t = 0$  and  $t = \tau'$ .

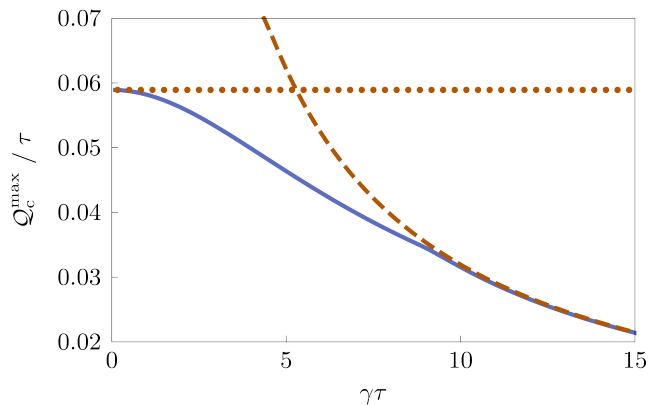


Figure 7. Quantum microcooler at slow and fast driving. The plot shows the maximum cooling power  $\mathcal{Q}_c^{\text{max}}/\tau$  in units of  $\gamma T_c$  as a function of the inverse adiabaticity parameter  $1/\varepsilon = \gamma\tau$ . In the limits  $\gamma\tau \gg 1$  and  $\gamma\tau \ll 1$ , the exact result from Sec. III C (solid line) approaches the adiabatic (dashed line) and high-frequency (dotted line) approximations, respectively. The parameters in this figure are the same as in Fig. 5a, i.e., the blue curves in both plots are identical.

### D. Semiclassical Microcooler Revisited

Before moving on to the full quantum regime, we now illustrate our approximation scheme for the semiclassical microcooler. For the sake of brevity, we here focus on maximum cooling power as our optimization criterion.

In the adiabatic limit, the reset stroke does not have to be considered explicitly and the optimal protocol  $\omega_t^{\text{P}}$  is given by (30) for  $0 \leq t \leq \tau$ . The two constants  $C_1$  and  $C_2$  thereby have to be chosen such that the extracted heat  $\mathcal{Q}_c[\omega_t] = \mathcal{Q}_c[C_1, C_2]$  becomes maximal. This condition is equivalent to optimizing the reset level  $\omega_\tau \in [\omega', \omega_{\text{max}}]$  of the control parameter and the initial value  $\lambda_0$  of the Lagrange multiplier, as described in the first part of Sec. IV B.

The resulting optimal cooling power is shown in Fig. 7 as a function of the dimensionless cycle time  $\gamma\tau$ , which corresponds to the inverse adiabaticity parameter  $1/\varepsilon$ . This plot confirms that our adiabatic response scheme is indeed accurate for  $\varepsilon \ll 1$ . In fact, the adiabatic approximation for  $\mathcal{Q}_c^{\text{max}}/\tau$  departs from the exact result obtained in Sec. III C only at  $1/\varepsilon \equiv \gamma\tau \simeq 10$ .

In the fast driving regime, the cooling power is maximized by a step protocol with the general form (45). The variational parameters  $\omega_0$ ,  $\omega_{\tau'}$  and  $\tau'$  can be determined exactly by maximizing the heat extraction (23) after inserting (43) and (45) and neglecting second order corrections in  $1/\varepsilon = \gamma\tau$ . We find that the optimal switching time is given by

$$\tau^*[\omega_0, \omega_{\tau'}] \equiv \frac{\sqrt{\Gamma_0^+ \Gamma_{\tau'}^+ - \Gamma_{\tau'}^+}}{\Gamma_0^+ - \Gamma_{\tau'}^+} \tau \quad (46)$$

as a function of the levels  $\omega_0$  and  $\omega_{\tau'}$  of the protocol  $\omega_t^{\text{HF}}$ . Here, we have used the abbreviation  $\Gamma_t^+ \equiv \Gamma^+[\omega_t]$ . The

optimal reset level is  $\omega_{\tau'}^* = \omega_{\max}$  and the optimal work level follows from maximizing the cooling power

$$\mathcal{Q}_c^{\max}/\tau = \max_{\omega_0} \{ \hbar\omega_0\gamma(1 - 2\tau^*[\omega_0, \omega_{\tau'}^*]/\tau) \}. \quad (47)$$

Note that this expression is independent of  $\varepsilon$ , since here we consider only the lowest order of the high-frequency expansion. Still, as shown in Fig. 7, the exact optimal cooling power approaches the constant value (47) for  $1/\varepsilon \lesssim 1$ , thus confirming the validity of our approximation scheme for the fast-driving regime.

## V. QUANTUM MICROCOOLER II – COHERENT REGIME

As a key application of our approximation methods, we will now show how the cooling power of the microcooler illustrated in Fig. 3 can be optimized in the full quantum regime. To this end, we first recall the qubit Hamiltonian (18),

$$H_t \equiv \frac{\hbar\Delta}{2}\sigma_x + \frac{\hbar\omega_t}{2}\sigma_z, \quad (48)$$

which describes the working system of this device. If the tunneling energy  $\Delta$  is not negligible, the periodic state that emerges due to cyclic variation of the control parameter  $\omega_t$  features coherences between the two energy levels of the qubit. The corresponding density matrix must therefore be parametrized in the general form

$$\rho_t \equiv \frac{1}{2}(\mathbb{1} + \mathbf{R}_t \cdot \boldsymbol{\sigma}), \quad (49)$$

where  $\boldsymbol{\sigma} \equiv (\sigma_x, \sigma_y, \sigma_z)^\top$  is the vector of Pauli matrices and the state vector  $\mathbf{R}_t$  fulfills the Bloch equation [17, 38]

$$\begin{aligned} \dot{\mathbf{R}}_t &= \mathbf{F}[\mathbf{R}_t, \Omega_t] \\ &\equiv \begin{bmatrix} -\Gamma_t^+ \frac{\Omega_t^2 + \Delta^2}{2\Omega_t^2} & -\omega_t & -\Gamma_t^+ \frac{\omega_t \Delta}{2\Omega_t^2} \\ \omega_t & -\frac{1}{2}\Gamma_t^+ & -\Delta \\ -\Gamma_t^+ \frac{\omega_t \Delta}{2\Omega_t^2} & \Delta & -\Gamma_t^+ \frac{2\Omega_t^2 - \Delta^2}{2\Omega_t^2} \end{bmatrix} \mathbf{R}_t - \frac{\Gamma_t^-}{\Omega_t} \begin{bmatrix} \Delta \\ 0 \\ \omega_t \end{bmatrix}. \end{aligned} \quad (50)$$

Here, the rates  $\Gamma_t^\pm \equiv \Gamma^\pm[\Omega_t]$  are defined as in (20) with  $\omega_t$  replaced by the instantaneous level splitting

$$\Omega_t \equiv \sqrt{\Delta^2 + \omega_t^2}, \quad (51)$$

which we will treat as the effective control parameter of the system from here onwards.

In order to extend our step-rate model to the coherent regime, we have to take into account that  $\Omega_t$  cannot vanish for finite  $\Delta$ . Therefore, the lower bound 0 in the coupling factor (22) has to be replaced with  $\Omega_{\min} = \Delta$ . Furthermore, also the threshold frequency  $\Omega'$ , which now takes the role of  $\omega'$  in the switching condition (21) for the reservoir temperature, has to be larger than  $\Delta$ .

Upon inserting (48) and (49) into the weak-coupling expression (4) for the instantaneous heat flux, the mean

heat extraction in the coherent regime becomes a functional of  $\Omega_t$ ,

$$\begin{aligned} \mathcal{Q}_c[\Omega_t] &\equiv \int_0^{\tau'} Q[\mathbf{R}_t, \Omega_t] dt \\ &\equiv - \int_0^{\tau'} \left( \frac{\hbar\Gamma_t^+}{2} (\Delta R_t^x + \omega_t R_t^z) + \frac{\hbar\Gamma_t^-}{2} \Omega_t \right) dt, \end{aligned} \quad (52)$$

which could, in principle, be optimized by applying the 3-step procedure of Sec. II B. This endeavor can be expected to be technically quite involved, since the periodicity constraint  $\mathbf{R}_\tau = \mathbf{R}_0$  now leads to three independent boundary conditions for the reset stroke, while only a single parameter is available to control the time-evolution of the state  $\mathbf{R}_t$ . However, to understand how the optimal performance of the microcooler changes in the quantum regime, it is sufficient to determine the impact of the tunneling energy  $\Delta$  on its maximum cooling power. For this purpose, it is not necessary to carry out the full optimization procedure. Instead, we can focus our analysis on the limits of slow and fast driving, where our approximation schemes enable a simple and physically transparent approach.

In the adiabatic-response regime, only the work stroke needs to be optimized [64]. To this end, we first integrate the canonical equations corresponding to the effective Hamiltonian

$$H_w[\mathbf{R}_t, \boldsymbol{\lambda}_t, \Omega_t] = Q[\mathbf{R}_t, \Omega_t] + \boldsymbol{\lambda}_t \cdot \mathbf{F}[\mathbf{R}_t, \Omega_t] \quad (53)$$

for the given initial conditions

$$\mathbf{R}_0 = \mathbf{R}_{\text{eq}}[\Omega_r] = -\frac{\Gamma^-[\Omega_r]}{\Gamma^+[\Omega_r]} \left( \frac{\Delta}{\Omega_r}, 0, \frac{\sqrt{\Omega_r^2 - \Delta^2}}{\Omega_r} \right)^\top \quad (54)$$

and  $\boldsymbol{\lambda}_0$ , see Appendix B. The parameters  $\Omega_r$  and  $\boldsymbol{\lambda}_0$  then have to be determined by maximizing the heat extraction  $\mathcal{Q}_c[\Omega_t] = \mathcal{Q}_c[\Omega_r, \boldsymbol{\lambda}_0]$ . This task is *a priori* challenging, since the initial Lagrange multipliers  $\lambda_0^x$  and  $\lambda_0^y$  are left unbounded by physical constraints. To overcome this problem, we use an iterative algorithm, which tracks the maximum of  $\mathcal{Q}_c[\Omega_r, \boldsymbol{\lambda}_0]$  as  $\Delta$  is increased in small steps starting from its semiclassical value  $\Delta = 0$ . This approach relies on the implicit assumption that the global maximum of the function  $\mathcal{Q}_c[\Omega_r, \boldsymbol{\lambda}_0]$  follows a continuous trajectory in the 4-dimensional space of variational parameters, which is justified *a posteriori* by the physical consistency of our results.

In the high-frequency regime, the cooling power is maximized by the step protocol

$$\Omega_t^{\text{HF}}[\tau', \Omega_0, \Omega_{\tau'}] = \Omega_0 + (\Omega_{\tau'} - \Omega_0)\Theta[t - \tau']. \quad (55)$$

As in the semiclassical case discussed in Sec. IV D, the variational parameters  $\tau'$ ,  $\Omega_0$  and  $\Omega_{\tau'}$  can be determined by maximizing the corresponding cooling power in first order with respect to  $1/\varepsilon = \gamma\tau$ . The resulting expression for  $\mathcal{Q}_c[\tau', \Omega_0, \Omega_{\tau'}]$  is rather involved and we do not show it here. The optimal variational parameters can however

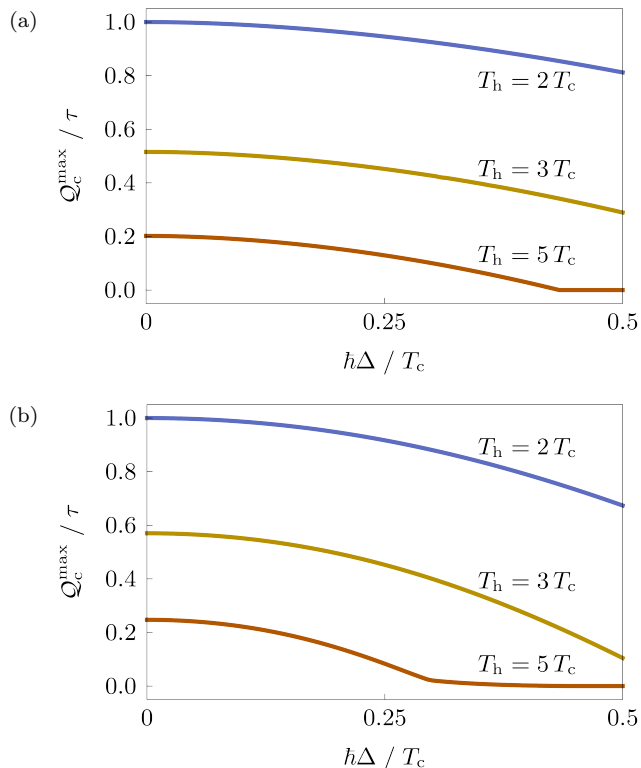


Figure 8. Optimal cooling power of the coherent microcooler as a function of the tunneling energy  $\Delta$ . (a) Maximum cooling power in the adiabatic regime ( $\gamma\tau = 10$ ) for different temperatures of the hot reservoir. (b) Maximum cooling power in the high-frequency regime (independent of  $\gamma\tau$ ). Here, we have used  $\Omega' = 1.5 T_c/\hbar$ ,  $\Omega_{\max} = 3 T_c/\hbar$  and  $\hbar\gamma = T_c$ . For comparison with the semiclassical model, the cooling power has been normalized with its value at  $\Delta = 0$  and  $T_h = 2 T_c$  in both plots.

be determined numerically. We note in particular that this optimization yields  $\Omega_{\tau'}^* = \Omega_{\max}$ .

Figure 8 shows the result of our analysis. In both the adiabatic and the high-frequency limit, the maximum cooling power monotonically decreases from its semiclassical value to 0 as  $\Delta$  increases. This behavior can be explained as follows. The tunneling energy  $\Delta$  corresponds to the minimal gap between the energy levels of the working system, see Fig. 3. Increasing this parameter reduces the amount of thermal energy that can be absorbed during the work stroke. As  $\Delta$  approaches a certain critical value, the capacity of the working system to pick up heat from the cold reservoir becomes too small for the device to operate properly. The optimal protocol then keeps the system practically in equilibrium at the low temperature  $T_c$  throughout the work stroke and the cooling power becomes zero. Since this general picture can be expected to prevail also for intermediate driving speed, we can conclude that to engineer a powerful microcooler, the tunneling energy of the qubit must be kept as small as possible.

## VI. DISCUSSION AND OUTLOOK

Our work provides a systematic scheme to optimize periodic driving protocols for mesoscopic two-stroke machines. Though developed here specifically for refrigerators, this general framework can easily be adapted to other types of thermal devices. Reciprocating heat engines, for example, use a periodically driven working system to convert thermal energy into mechanical power [48, 53, 65, 66]. Within our two-stroke approach, this process can be described as a reversed cooling cycle. That is, the system picks up heat from a hot reservoir in the first stroke and returns to its initial state while being in contact with a cold reservoir in the second stroke. To achieve optimal performance, the engine has to generate as much work output as possible from a given amount of thermal input energy. Owing to the first law, this optimization criterion is equivalent to minimizing the dissipated heat during the reset while keeping the heat uptake during the work stroke fixed. The corresponding optimal control protocol can thus be determined using the 3-step procedure of Sec. II C.

The performance figures of mesoscopic thermal devices, such as power and efficiency, can generally not be optimized simultaneously. Instead, they are subject to universal trade-off relations as several recent studies have shown [60, 61, 67, 68]. As one of its potential key applications, our two-stroke scheme makes it possible to test the quality of these constraints under practical conditions. Furthermore, covering both classical and quantum systems, the framework developed in this article might open a new avenue to systematically explore the impact of coherence on the performance of thermodynamic cycles, a central topic in quantum thermodynamics, see for example Refs. [24, 53, 68–73].

To facilitate future investigations in these directions, our scheme can be combined with a variety of dynamical approximation methods. In Sec. IV, for example, we have shown how adiabatic and high-frequency expansion techniques can be included. To this end, we have solved the dynamical constraint perturbatively assuming that the external driving is either slow or fast compared to the relaxation time of the working system. This approach makes it possible to circumvent the use of Lagrange multipliers and thus reduces the amount of dynamical parameters in the optimization problem. An alternative strategy could use the variational equations in the extended parameter space as a starting point. Specifically, the canonical structure of these equations makes it possible to implement a variety of tools that were originally developed for the description of classical Hamiltonian systems including adiabatic gauge potentials [74], shortcuts to adiabaticity [75, 76] or non-linear generalizations of the Magnus expansion [77].

Integrating such advanced methods into our general framework will inevitably require a reliable reference to assess their practicality and accuracy. Such a testbed is provided in Sec. III, where we have developed a simple

and physically transparent model of a quantum microcooler, whose optimal operation cycle can be determined exactly. In fact, this case study provides both a demonstration that our theoretical framework is directly applicable to ongoing experiments with engineered quantum systems and a valuable benchmark for further advances in theoretical optimization methods.

### ACKNOWLEDGMENTS

We thank J. P. Pekola for useful discussions. K. B. acknowledges support from the Academy of Finland (Contract No. 296073). This work was supported by the Academy of Finland (projects No. 308515 and 312299). All authors are associated with the Centre for Quantum Engineering at Aalto University.

### Appendix A: Alternative Optimization Scheme for the Semiclassical Microcooler

In Sec. III C, we have derived the optimal work protocol (40) for the semiclassical microcooler by enforcing the dynamical constraint (20) with a Lagrange multiplier. Here, we present an alternative method to obtain the result (40), which exploits the one-to-one correspondence between the control parameter and the derivative of the state variable in this model.

We proceed as follows. First, solving Eq. (20) for  $\omega_t$  yields

$$\omega_t = \frac{T_c}{\hbar} \ln \left[ \frac{\gamma(1-R_t)}{\dot{R}_t + \gamma(1+R_t)} \right]. \quad (\text{A1})$$

Upon inserting this expression into (23), the objective functional becomes

$$\mathcal{Q}_c[R_t] = \int_0^{\tau'} Q[R_t, \dot{R}_t] dt, \quad (\text{A2})$$

where the effective Lagrangian

$$Q[R_t, \dot{R}_t] \equiv \frac{T_c}{2} \dot{R}_t \ln \left[ \frac{\gamma(1-R_t)}{\dot{R}_t + \gamma(1+R_t)} \right] \quad (\text{A3})$$

does not explicitly depend on time. Consequently, the corresponding effective Hamiltonian is a constant of motion given by

$$4\gamma C_1 \equiv \frac{\dot{R}_t^2}{R_t + \gamma(1+R_t)}. \quad (\text{A4})$$

Using (20),  $C_1$  can be expressed in terms of the initial values  $R_0$  and  $\omega_0$  as

$$C_1 = \frac{1}{1-R_0} \left( R_0 \cosh \left[ \frac{\hbar\omega_0}{2T_c} \right] + \sinh \left[ \frac{\hbar\omega_0}{2T_c} \right] \right)^2. \quad (\text{A5})$$

This expression shows that  $C_1$  is non-negative. Furthermore, for  $C_1 = 0$ , (A4) and (A5) imply  $R_t = R_0 = -\tanh[\hbar\omega_0/(2T_c)]$  and  $\omega_t = \omega_0$ , that is, the system is in equilibrium throughout the cycle and the average heat extraction (A2) becomes zero.

Second, solving (A4) for  $\dot{R}_t$  gives

$$\dot{R}_t = 2\gamma(C_1 \pm \sqrt{C_1(C_1 + 1 + R_t)}), \quad (\text{A6})$$

where only the positive branch of the square root leads to  $\dot{R}_t > 0$  and thus positive heat extraction. Since we require that the control parameter  $\omega_t$ , which is given by (A1) in terms of  $R_t$ , does not jump during the work stroke, both  $R_t$  and  $\dot{R}_t$  must be continuous. We can thus neglect the negative branch in (A6). Note that this choice implies the constraint  $\dot{R}_0 = F[R_0, \omega_0] > 0$  on the initial values  $R_0$  and  $\omega_0$ , cf. (29) and (37).

Third, solving the differential equation (A6) under this condition yields

$$R_t^p = -1 + C_1 \left( (1 + W_{-1}[C_2 e^{-\gamma t}])^2 - 1 \right), \quad (\text{A7})$$

where the dimensionless constant  $C_2$  is given by

$$C_2 = W^{-1} \left[ \frac{2(1-R_0)}{(1+R_0)e^{\hbar\omega_0/(kT_c)} - (1-R_0)} \right], \quad (\text{A8})$$

with  $W^{-1}[x] \equiv xe^x$ . Thus, we have recovered the result (31) of the main text.

### Appendix B: Optimal Work Stroke of the Coherent Microcooler

The optimal work stroke of the coherent microcooler discussed in Sec. V is described by the effective Hamiltonian

$$\begin{aligned} H_w[\mathbf{R}_t, \boldsymbol{\lambda}_t, \Omega_t] & \quad (\text{B1}) \\ &= \frac{T_c}{2} \boldsymbol{\lambda}_t \cdot \mathbf{F}[\mathbf{R}_t, \Omega_t] - \frac{\hbar\Gamma_t^+}{2} (\Delta R_t^x + \omega_t R_t^z) - \frac{\hbar\Gamma_t^-}{2} \Omega_t, \end{aligned}$$

where we rescaled the Lagrange multipliers  $\boldsymbol{\lambda}_t$  by a factor of  $T_c/2$  compared with (53) for convenience. The corresponding canonical equations for the state variables and Lagrange multipliers are given by

$$\dot{\mathbf{R}}_t = \mathbf{F}[\mathbf{R}_t, \Omega_t] \quad (\text{B2})$$

$$\equiv \begin{bmatrix} -\Gamma_t^+ \frac{\Omega_t^2 + \Delta^2}{2\Omega_t^2} & -\omega_t & -\Gamma_t^+ \frac{\omega_t \Delta}{2\Omega_t^2} \\ \omega_t & -\frac{1}{2}\Gamma_t^+ & -\Delta \\ -\Gamma_t^+ \frac{\omega_t \Delta}{2\Omega_t^2} & \Delta & -\Gamma_t^+ \frac{2\Omega_t^2 - \Delta^2}{2\Omega_t^2} \end{bmatrix} \mathbf{R}_t - \frac{\Gamma_t^-}{\Omega_t} \begin{bmatrix} \Delta \\ 0 \\ \omega_t \end{bmatrix}$$

and

$$\dot{\boldsymbol{\lambda}}_t = \begin{bmatrix} \Gamma_t^+ \frac{\Omega_t^2 + \Delta^2}{2\Omega_t^2} & -\omega_t & \Gamma_t^+ \frac{\omega_t \Delta}{2\Omega_t^2} \\ \omega_t & \frac{1}{2}\Gamma_t^+ & -\Delta \\ \Gamma_t^+ \frac{\omega_t \Delta}{2\Omega_t^2} & \Delta & \Gamma_t^+ \frac{2\Omega_t^2 - \Delta^2}{2\Omega_t^2} \end{bmatrix} \boldsymbol{\lambda}_t + \frac{\hbar\Gamma_t^+}{T_c} \begin{bmatrix} \Delta \\ 0 \\ \omega_t \end{bmatrix}, \quad (\text{B3})$$

respectively. We recall that the energy bias  $\omega_t$  and the level splitting  $\Omega_t$  are related by  $\omega_t = \sqrt{\Omega_t^2 - \Delta^2}$ .

The evolution equations (B2) and (B3) are coupled by the algebraic constraint

$$\frac{\partial}{\partial \Omega_t} H_w[\mathbf{R}_t, \boldsymbol{\lambda}_t, \Omega_t] = 0. \quad (\text{B4})$$

This differential-algebraic system could, in principle, be integrated by solving the algebraic constraint for  $\Omega_t = \Omega[\mathbf{R}_t, \boldsymbol{\lambda}_t]$ . Equations (B2) and (B3) would then become an ordinary system of differential equations, which could be integrated using standard techniques. This approach has been used for the semiclassical microcooler in Sec. III C. However, owing to its complicated structure, solving the constraint (B4) for  $\Omega_t$  is hard to implement in practice.

Instead, it is more convenient to transform the Bloch equations into a co-rotating frame. To this end, we define the transformed Bloch vector  $\mathbf{r}_t$  by replacing the static parametrization (49) with

$$\rho_t \equiv \frac{1}{2} V_t (\mathbb{1} + \mathbf{r}_t \cdot \boldsymbol{\sigma}) V_t^\dagger. \quad (\text{B5})$$

Here,  $V_t$  denotes the unitary matrix

$$V_t \equiv \begin{pmatrix} \cos[\varphi_t/2] & -\sin[\varphi_t/2] \\ \sin[\varphi_t/2] & \cos[\varphi_t/2] \end{pmatrix} \quad (\text{B6})$$

with  $\tan[\varphi_t] \equiv \Delta/\omega_t$ , which diagonalizes the instantaneous Hamiltonian  $H_t$ . In fact, the vectors  $\mathbf{R}_t$  and  $\mathbf{r}_t$  differ by a rotation in the  $x$ - $z$  plane by the angle  $\varphi_t$ . This change of coordinates separates the population and the coherence degrees of freedom of the density matrix, which

are now parametrized by  $r_t^z$  and  $r_t^{x,y}$ , respectively. Note that, in contrast to  $\mathbf{R}_t$ , the transformed Bloch vector  $\mathbf{r}_t$  is not continuous at the jumps of the control protocol  $\Omega_t$ ; if  $V_{t-dt}$  and  $V_t$  are the rotation operators corresponding to the Hamiltonian before and after the jump, respectively, the accompanying jump in  $\mathbf{r}_t$  is determined by the condition

$$r_t^k = \text{tr}[V_t^\dagger V_{t-dt} (\mathbf{r}_{t-dt} \cdot \boldsymbol{\sigma}) V_{t-dt}^\dagger V_t \sigma_k] / 2. \quad (\text{B7})$$

In the following, we will show how the optimal work protocol can be calculated in the rotating frame. To this end, we first observe that the transformed Bloch equation reads

$$\dot{\mathbf{r}}_t = \begin{bmatrix} -\Gamma_t^+/2 & -\Omega_t & -\dot{\varphi}[\Omega_t, \dot{\Omega}_t] \\ \Omega_t & -\Gamma_t^+/2 & 0 \\ \dot{\varphi}[\Omega_t, \dot{\Omega}_t] & 0 & -\Gamma_t^+ \end{bmatrix} \mathbf{r}_t - \begin{bmatrix} 0 \\ 0 \\ \Gamma_t^- \end{bmatrix}. \quad (\text{B8})$$

As an artifact of the time-dependent parametrization (B5), the right hand side of (B8) now depends on the time-derivative of the control parameter,  $\dot{\Omega}_t$ . Our general optimization scheme can, however, still be applied without major modifications since  $\dot{\Omega}_t$  has no physical significance here.

The transformed vector of Lagrange multipliers,  $\boldsymbol{\Lambda}_t$ , satisfies the evolution equation

$$\dot{\boldsymbol{\Lambda}}_t = \begin{bmatrix} \Gamma_t^+/2 & -\Omega_t & -\dot{\varphi}[\Omega_t, \dot{\Omega}_t] \\ \Omega_t & \Gamma_t^+/2 & 0 \\ \dot{\varphi}[\Omega_t, \dot{\Omega}_t] & 0 & \Gamma_t^+ \end{bmatrix} \boldsymbol{\Lambda}_t + \frac{\hbar \Omega_t}{T_c} \begin{bmatrix} 0 \\ 0 \\ \Gamma_t^+ \end{bmatrix} \quad (\text{B9})$$

in the rotating frame and the algebraic constraint (B4) becomes

$$\begin{aligned} & \frac{\hbar \Delta}{T_c} \left\{ 2\Lambda_t^x (1 - e^{-W_t}) + (2W_t r_t^x + \Lambda_t^z r_t^x + \Lambda_t^x r_t^z) (1 + e^{-W_t}) + \frac{2T_c}{\hbar \gamma} W_t (\Lambda_t^y r_t^z - \Lambda_t^z r_t^y) \right\} \\ & = \frac{\hbar \Omega_t}{T_c} \frac{\hbar \omega_t}{T_c} \left\{ 2(1 + r_t^z) - \frac{2T_c}{\hbar \gamma} (\Lambda_t^y r_t^x - \Lambda_t^x r_t^y) - e^{-W_t} \left( 2(1 - r_t^z)(1 - W_t - \Lambda_t^z) + \Lambda_t^x r_t^x + \Lambda_t^y r_t^y \right) \right\} \end{aligned} \quad (\text{B10})$$

in the new variables, where  $W_t = \hbar \Omega_t / T_c$ .

In order to obtain a closed system of differential equations, we have to express  $\dot{\Omega}_t$  in terms of  $\mathbf{r}_t$ ,  $\boldsymbol{\Lambda}_t$  and  $\Omega_t$ . To this end, we take the time-derivative of the algebraic constraint (B10) and then use (B8) and (B9) to eliminate  $\dot{\mathbf{r}}_t$  or  $\dot{\boldsymbol{\Lambda}}_t$ . The resulting expression can be rewritten in the form

$$\dot{\Omega}_t = \dot{\Omega}[\mathbf{r}_t, \boldsymbol{\Lambda}_t, \Omega_t]. \quad (\text{B11})$$

The relation (B11) enables the following strategy to

find the optimal time evolution. We first choose initial values  $(\mathbf{r}_0, \boldsymbol{\Lambda}_0, \Omega_0)$ , which are compatible with the algebraic constraint (B10). For this purpose, we note that (B10) is a linear equation in  $\mathbf{r}_t$  and  $\boldsymbol{\Lambda}_t$ . Therefore, it is straightforward to determine, for example,  $\Lambda_0^z$  if all other initial values are given. The equations (B8), (B9) and (B11) then form an autonomous system of seven first-order differential equations, which can be treated as a standard initial value problem. By construction, the resulting solution complies with the algebraic constraint (B10) at any time  $t \geq 0$ .



- 
- [1] Francesco Giazotto, Tero T. Heikkilä, Arttu Luukanen, Alexander M. Savin, and Jukka P. Pekola, “Opportunities for mesoscopics in thermometry and refrigeration: Physics and applications,” *Rev. Mod. Phys.* **78**, 217–274 (2006).
- [2] Noah Linden, Sandu Popescu, and Paul Skrzypczyk, “How Small Can Thermal Machines Be? The Smallest Possible Refrigerator,” *Phys. Rev. Lett.* **105**, 130401 (2010).
- [3] Juha T. Muhonen, Matthias Meschke, and Jukka P. Pekola, “Micrometre-scale refrigerators,” *Rep. Prog. Phys.* **75**, 046501 (2012).
- [4] H. Courtois, F. W. J. Hekking, H. Q. Nguyen, and C. B. Winkelmann, “Electronic Coolers Based on Superconducting Tunnel Junctions: Fundamentals and Applications,” *J. Low Temp. Phys.* **175**, 799–812 (2014).
- [5] Jukka P. Pekola, “Towards quantum thermodynamics in electronic circuits,” *Nat. Phys.* **11**, 118 (2015).
- [6] M. H. Devoret and R. J. Schoelkopf, “Superconducting Circuits for Quantum Information: An Outlook,” *Science* **339**, 1169–1174 (2013).
- [7] R. Barends, J. Kelly, A. Megrant, A. Veitia, D. Sank, E. Jeffrey, T. C. White, J. Mutus, A. G. Fowler, B. Campbell, Y. Chen, Z. Chen, B. Chiaro, A. Dunsworth, C. Neill, P. O’Malley, P. Roushan, A. Vainsencher, J. Wenner, A. N. Korotkov, A. N. Cleland, and John M. Martinis, “Superconducting quantum circuits at the surface code threshold for fault tolerance,” *Nature* **508**, 500–503 (2014).
- [8] J. Kelly, R. Barends, A. G. Fowler, A. Megrant, E. Jeffrey, T. C. White, D. Sank, J. Y. Mutus, B. Campbell, Yu Chen, Z. Chen, B. Chiaro, A. Dunsworth, I.-C. Hoi, C. Neill, P. J. J. O’Malley, C. Quintana, P. Roushan, A. Vainsencher, J. Wenner, A. N. Cleland, and John M. Martinis, “State preservation by repetitive error detection in a superconducting quantum circuit,” *Nature* **519**, 66–69 (2015).
- [9] M. Grajcar, S. H. W. van der Ploeg, A. Izmailov, E. Il’ichev, H.-G. Meyer, A. Fedorov, A. Shnirman, and Gerd Schön, “Sisyphus cooling and amplification by a superconducting qubit,” *Nat. Phys.* **4**, 612–616 (2008).
- [10] Francesco Giazotto and María José Martínez-Pérez, “The Josephson heat interferometer,” *Nature* **492**, 401–405 (2012).
- [11] Patrick P. Hofer, Martí Perarnau-Llobet, Jonatan Bohr Brask, Ralph Silva, Marcus Huber, and Nicolas Brunner, “Autonomous quantum refrigerator in a circuit QED architecture based on a Josephson junction,” *Phys. Rev. B* **94**, 235420 (2016).
- [12] Matti Partanen, Kuan Yen Tan, Joonas Govenius, Russell E. Lake, Miika K. Mäkelä, Tuomo Tanttu, and Mikko Möttönen, “Quantum-limited heat conduction over macroscopic distances,” *Nat. Phys.* **12**, 460–464 (2016).
- [13] Antonio Fornieri, Christophe Blanc, Riccardo Bosisio, Sophie D’Ambrosio, and Francesco Giazotto, “Nanoscale phase engineering of thermal transport with a Josephson heat modulator,” *Nat. Nanotechnol.* **11**, 258–262 (2016).
- [14] Kuan Yen Tan, Matti Partanen, Russell E. Lake, Joonas Govenius, Shumpei Masuda, and Mikko Möttönen, “Quantum-circuit refrigerator,” *Nat. Commun.* **8**, 15189 (2017).
- [15] Alberto Ronzani, Bayan Karimi, Jordan Senior, Yu-Cheng Chang, Joonas T. Peltonen, ChiiDong Chen, and Jukka P. Pekola, “Tunable photonic heat transport in a quantum heat valve,” *Nat. Phys.* **14**, 991–995 (2018).
- [16] H. T. Quan, Y. D. Wang, Yu-xi Liu, C. P. Sun, and Franco Nori, “Maxwell’s Demon Assisted Thermodynamic Cycle in Superconducting Quantum Circuits,” *Phys. Rev. Lett.* **97**, 180402 (2006).
- [17] A. O. Niskanen, Y. Nakamura, and J. P. Pekola, “Information entropic superconducting microcooler,” *Phys. Rev. B* **76**, 174523 (2007).
- [18] Armen E. Allahverdyan, Karen Hovhannisyanyan, and Guenter Mahler, “Optimal refrigerator,” *Phys. Rev. E* **81**, 051129 (2010).
- [19] Ronnie Kosloff and Tova Feldmann, “Optimal performance of reciprocating demagnetization quantum refrigerators,” *Phys. Rev. E* **82**, 011134 (2010).
- [20] Tova Feldmann and Ronnie Kosloff, “Short time cycles of purely quantum refrigerators,” *Phys. Rev. E* **85**, 051114 (2012).
- [21] M. Kolář, D. Gelbwaser-Klimovsky, R. Alicki, and G. Kurizki, “Quantum Bath Refrigeration towards Absolute Zero: Challenging the Unattainability Principle,” *Phys. Rev. Lett.* **109**, 090601 (2012).
- [22] Y. Izumida, K. Okuda, A. Calvo Hernández, and J. M. M. Roco, “Coefficient of performance under optimized figure of merit in minimally nonlinear irreversible refrigerator,” *EPL* **101**, 10005 (2013).
- [23] Michele Campisi, Jukka Pekola, and Rosario Fazio, “Nonequilibrium fluctuations in quantum heat engines: Theory, example, and possible solid state experiments,” *New J. Phys.* **17**, 035012 (2015).
- [24] Raam Uzdin, Amikam Levy, and Ronnie Kosloff, “Equivalence of Quantum Heat Machines, and Quantum-Thermodynamic Signatures,” *Phys. Rev. X* **5**, 031044 (2015).
- [25] Obinna Abah and Eric Lutz, “Optimal performance of a quantum Otto refrigerator,” *EPL* **113**, 60002 (2016).
- [26] Karel Proesmans, Yannik Dreher, Momčilo Gavrilov, John Bechhoefer, and Christian Van den Broeck, “Brownian Duet: A Novel Tale of Thermodynamic Efficiency,” *Phys. Rev. X* **6**, 041010 (2016).
- [27] Jukka P. Pekola, Bayan Karimi, George Thomas, and Dmitri V. Averin, “Supremacy of incoherent sudden cycles,” (2018), arXiv:1812.10933 [quant-ph].
- [28] T. Schmiedl and U. Seifert, “Efficiency at maximum power: An analytically solvable model for stochastic heat engines,” *EPL* **81**, 20003 (2007).
- [29] M. Esposito, R. Kawai, K. Lindenberg, and C. Van den Broeck, “Finite-time thermodynamics for a single-level quantum dot,” *EPL* **89**, 20003 (2010).
- [30] Bjarne Andresen, “Current Trends in Finite-Time Thermodynamics,” *Angew. Chem. Int. Ed.* **50**, 2690–2704 (2011).
- [31] Viktor Holubec, “An exactly solvable model of a stochastic heat engine: Optimization of power, power fluctuations and efficiency,” *J. Stat. Mech.* **2014**, P05022 (2014).
- [32] Andreas Dechant, Nikolai Kiesel, and Eric Lutz, “All-Optical Nanomechanical Heat Engine,” *Phys. Rev. Lett.* **114**, 183602 (2015).

- [33] Kay Brandner, Keiji Saito, and Udo Seifert, “Thermodynamics of micro- and nano-systems driven by periodic temperature variations,” *Phys. Rev. X* **5**, 031019 (2015).
- [34] Michael Bauer, Kay Brandner, and Udo Seifert, “Optimal performance of periodically driven, stochastic heat engines under limited control,” *Phys. Rev. E* **93**, 042112 (2016).
- [35] A. Dechant, N. Kiesel, and E. Lutz, “Underdamped stochastic heat engine at maximum efficiency,” *EPL* **119**, 50003 (2017).
- [36] Raam Uzdin and Ronnie Kosloff, “Universal features in the efficiency at maximal work of hot quantum Otto engines,” *EPL* **108**, 40001 (2014).
- [37] Kay Brandner and Udo Seifert, “Periodic thermodynamics of open quantum systems,” *Phys. Rev. E* **93**, 062134 (2016).
- [38] B. Karimi and J. P. Pekola, “Otto refrigerator based on a superconducting qubit: Classical and quantum performance,” *Phys. Rev. B* **94**, 184503 (2016).
- [39] Nishchay Suri, Felix C. Binder, Bhaskaran Muralidharan, and Sai Vinjanampathy, “Speeding up thermalisation via open quantum system variational optimisation,” *Eur. Phys. J. Spec. Top.* **227**, 203–216 (2018).
- [40] Vasco Cavina, Andrea Mari, Alberto Carlini, and Vittorio Giovannetti, “Optimal thermodynamic control in open quantum systems,” *Phys. Rev. A* **98**, 012139 (2018).
- [41] Paolo Andrea Erdman, Vasco Cavina, Rosario Fazio, Fabio Taddei, and Vittorio Giovannetti, “Maximum Power and Corresponding Efficiency for Two-Level Quantum Heat Engines and Refrigerators,” (2018), arXiv:1812.05089 [quant-ph].
- [42] Donald E. Kirk, *Optimal Control Theory: An Introduction* (Courier Corporation, 2004).
- [43] F. Boldt, K. H. Hoffmann, P. Salamon, and R. Kosloff, “Time-optimal processes for interacting spin systems,” *EPL* **99**, 40002 (2012).
- [44] Sebastian Deffner, “Optimal control of a qubit in an optical cavity,” *J. Phys. B* **47**, 145502 (2014).
- [45] Ronnie Kosloff and Yair Rezek, “The quantum harmonic Otto cycle,” *Entropy* **19**, 136 (2017).
- [46] L. S. Pontryagin, V. G. Boltyanskii, R. V. Gamkrelidze, and E. F. Mishchenko, *The Mathematical Theory of Optimal Processes* (J. Wiley and Sons, New York, 1962).
- [47] Udo Seifert, “Stochastic thermodynamics, fluctuation theorems and molecular machines,” *Rep. Prog. Phys.* **75**, 126001 (2012).
- [48] Giuliano Benenti, Giulio Casati, Keiji Saito, and Robert S. Whitney, “Fundamental aspects of steady-state conversion of heat to work at the nanoscale,” *Phys. Rep.* **694**, 1–124 (2017).
- [49] David Gelbwaser-Klimovsky, Wolfgang Niedenzu, and Gershon Kurizki, “Chapter Twelve - Thermodynamics of Quantum Systems Under Dynamical Control,” in *Advances In Atomic, Molecular, and Optical Physics*, Vol. 64, edited by Ennio Arimondo, Chun C. Lin, and Susanne F. Yelin (Academic Press, 2015) pp. 329–407.
- [50] Herbert Spohn and Joel L. Lebowitz, “Irreversible Thermodynamics for Quantum Systems Weakly Coupled to Thermal Reservoirs,” *Adv. Chem. Phys.* **38**, 109–142 (1978).
- [51] R. Alicki, “The quantum open system as a model of the heat engine,” *J. Phys. A* **12**, L103 (1979).
- [52] Eitan Geva and Ronnie Kosloff, “Three-level quantum amplifier as a heat engine: A study in finite-time thermodynamics,” *Phys. Rev. E* **49**, 3903–3918 (1994).
- [53] Sai Vinjanampathy and Janet Anders, “Quantum thermodynamics,” *Contemp. Phys.* **57**, 545–579 (2016).
- [54] Herbert Goldstein, Charles P. Poole, and John L. Safko, *Classical Mechanics* (Addison Wesley, 2002).
- [55] An alternative way to see that  $\omega_t^n[\mathbf{R}_0, \boldsymbol{\lambda}_0] = \omega_t^p[\mathbf{R}_0, \boldsymbol{\lambda}_0]$  must hold during the work stroke is to observe that the protocol minimizing the effective input  $Q_h$  for fixed effective output  $Q_c^*$  simultaneously maximizes the output for fixed input.
- [56] Note that we have rescaled the objective functional, giving the Lagrange multiplier the same dimension as  $\omega$ .
- [57] Since the work stroke has a maximum duration, there are admissible initial conditions for which there is no intersection. We handle this case in practice by allowing for an intermediate time in which the system is decoupled from both reservoirs and the system state remains constant. We find that the protocol yielding the maximal average cooling power never decouples the system from both reservoirs.
- [58] Ciyu Zhu, Richard H. Byrd, Peihuang Lu, and Jorge Nocedal, “Algorithm 778: L-BFGS-B: Fortran Subroutines for Large-scale Bound-constrained Optimization,” *ACM Trans. Math. Softw.* **23**, 550–560 (1997).
- [59] Note that, in order to account for reset protocols with  $\omega_{r'} > \omega'$ ,  $\tau_1$  must be allowed to become smaller than  $\tau'$ .
- [60] Naoto Shiraishi, Keiji Saito, and Hal Tasaki, “Universal Trade-Off Relation between Power and Efficiency for Heat Engines,” *Phys. Rev. Lett.* **117**, 190601 (2016).
- [61] Patrick Pietzonka and Udo Seifert, “Universal Trade-Off between Power, Efficiency, and Constancy in Steady-State Heat Engines,” *Phys. Rev. Lett.* **120**, 190602 (2018).
- [62] Naoto Shiraishi and Keiji Saito, “Fundamental Relation Between Entropy Production and Heat Current,” *J. Stat. Phys.* **174**, 433–468 (2019).
- [63] Vasco Cavina, Andrea Mari, and Vittorio Giovannetti, “Slow Dynamics and Thermodynamics of Open Quantum Systems,” *Phys. Rev. Lett.* **119**, 050601 (2017).
- [64] We note that the adiabatic approximation to apply here, the relaxation time  $1/\gamma$  has to be large compared to both the cycle time  $\tau$  and the time scale of the coherent oscillations.
- [65] H. T. Quan, Y. X. Liu, C. P. Sun, and Franco Nori, “Quantum thermodynamic cycles and quantum heat engines,” *Phys. Rev. E* **76**, 031105 (2007).
- [66] Ronnie Kosloff, “Quantum thermodynamics: A dynamical viewpoint,” *Entropy* **15**, 2100–2128 (2013).
- [67] Björn Sothmann, Rafael Sánchez, and Andrew N Jordan, “Thermoelectric energy harvesting with quantum dots,” *Nanotechnology* **26**, 032001 (2014).
- [68] Kay Brandner, Michael Bauer, and Udo Seifert, “Universal Coherence-Induced Power Losses of Quantum Heat Engines in Linear Response,” *Phys. Rev. Lett.* **119**, 170602 (2017).
- [69] Nicolas Brunner, Marcus Huber, Noah Linden, Sandu Popescu, Ralph Silva, and Paul Skrzypczyk, “Entanglement enhances cooling in microscopic quantum refrigerators,” *Phys. Rev. E* **89**, 032115 (2014).
- [70] J. Roßnagel, O. Abah, F. Schmidt-Kaler, K. Singer, and E. Lutz, “Nanoscale Heat Engine Beyond the Carnot Limit,” *Phys. Rev. Lett.* **112**, 030602 (2014).
- [71] Matteo Lostaglio, Kamil Korzekwa, David Jennings, and Terry Rudolph, “Quantum Coherence, Time-Translation

- Symmetry, and Thermodynamics,” *Phys. Rev. X* **5**, 021001 (2015).
- [72] Piotr Ćwikliński, Michał Studziński, Michał Horodecki, and Jonathan Oppenheim, “Limitations on the Evolution of Quantum Coherences: Towards Fully Quantum Second Laws of Thermodynamics,” *Phys. Rev. Lett.* **115**, 210403 (2015).
- [73] Jan Klaers, Stefan Faelt, Atac Imamoglu, and Emre Togan, “Squeezed Thermal Reservoirs as a Resource for a Nanomechanical Engine beyond the Carnot Limit,” *Phys. Rev. X* **7**, 031044 (2017).
- [74] Michael Kolodrubetz, Dries Sels, Pankaj Mehta, and Anatoli Polkovnikov, “Geometry and non-adiabatic response in quantum and classical systems,” *Phys. Rep.* **697**, 1–87 (2017).
- [75] Christopher Jarzynski, “Generating shortcuts to adiabaticity in quantum and classical dynamics,” *Phys. Rev. A* **88**, 040101 (2013).
- [76] Sebastian Deffner, Christopher Jarzynski, and Adolfo del Campo, “Classical and Quantum Shortcuts to Adiabaticity for Scale-Invariant Driving,” *Phys. Rev. X* **4**, 021013 (2014).
- [77] S. Blanes, F. Casas, J. A. Oteo, and J. Ros, “The Magnus expansion and some of its applications,” *Phys. Rep.* **470**, 151–238 (2009).